Naval Research Laboratory

Stennis Space Center, MS 39529-5004

NRL/MR/7320--12-9361

Validation Test Report for a Genetic Algorithm in the Glider Observation STrategies (GOST 1.0) Project: Sensitivity Studies

Lucy F. Smedstad

Ocean Dynamics and Prediction Branch
Oceanography Division

Kevin D. Heaney

Ocean Acoustical Services and Instrumentation Systems, Inc.
Lexington, Massachusetts

Germana Peggion

University of New Orleans
New Orleans, Louisiana

Charlie N. Barron

Ocean Dynamics and Prediction Branch
Oceanography Division

Emanuel Coelho

University of New Orleans
New Orleans, Louisiana

August 15, 2012

REPORT DOCUMENTATION PAGE

Form Approved
OMB No. 0704-0188

1. REPORT DATE *(DD-MM-YYYY)*
15-08-2012

2. REPORT TYPE
Memorandum Report

3. DATES COVERED *(From - To)*

4. TITLE AND SUBTITLE
Validation Test Report for a Genetic Algorithm in the Glider Observation STrategies (GOST 1.0) Project: Sensitivity Studies

5a. CONTRACT NUMBER

5b. GRANT NUMBER

5c. PROGRAM ELEMENT NUMBER
0603207N

6. AUTHOR(S)
Lucy F. Smedstad, Kevin D. Heaney,* Germana Peggion,‡ Charlie N. Barron, and Emanuel Coelho‡

5d. PROJECT NUMBER

5e. TASK NUMBER

5f. WORK UNIT NUMBER
73-5091-12-5

7. PERFORMING ORGANIZATION NAME(S) AND ADDRESS(ES)
Naval Research Laboratory
Oceanography Division
Stennis Space Center, MS 39529-5004

8. PERFORMING ORGANIZATION REPORT NUMBER
NRL/MR/7320--12-9361

9. SPONSORING / MONITORING AGENCY NAME(S) AND ADDRESS(ES)
Space & Naval Warfare Systems Command
2451 Crystal Drive
Arlington, VA 22245-5200

10. SPONSOR / MONITOR'S ACRONYM(S)
SPAWAR

11. SPONSOR / MONITOR'S REPORT NUMBER(S)

12. DISTRIBUTION / AVAILABILITY STATEMENT
Approved for public release; distribution is unlimited.

13. SUPPLEMENTARY NOTES
*Ocean Acoustical Services and Instrumentation Systems (OASIS), Inc., 5 Militia Drive, Lexington, MA 02421-4706
‡University of New Orleans, 2000 Lakeshore Drive, New Orleans, LA 70148

14. ABSTRACT

A suite of sensors in an oceanographic area of interest may be optimized with the use of a Genetic Algorithm (GA). The Environmental Measurements Path Planner (EMPath) executes a GA to generate optimal search plans for a suite of sensors based upon constituent cost-functions (CCF) contained in an input netcdf file. This GA software is incorporated to interface with the Relocatable Circulation Prediction System (RELO) under the Glider Observation Strategies (GOST) Project.

This Validation Test Report (VTR) explores the sensitivity of a RELO to different Observation System Simulation Experiments (OSSEs) with simulated gliders in an area. Results are presented from a real-time exercise using the system, the Maritime Rapid Environmental Assessment of 2010 (MREA10), that include a full feedback cycle to guide a glider and assimilate the collected data back into the model.

15. SUBJECT TERMS
Gliders; Glider sampling; Genetic algorithm; Ocean modeling; Optimal coverage; Sampling platforms; Target area

16. SECURITY CLASSIFICATION OF: a. REPORT	b. ABSTRACT	c. THIS PAGE	17. LIMITATION OF ABSTRACT	18. NUMBER OF PAGES	19a. NAME OF RESPONSIBLE PERSON
Unclassified Unlimited	Unclassified Unlimited	Unclassified Unlimited	Unclassified Unlimited	44	Lucy Smedstad
					19b. TELEPHONE NUMBER *(include area code)* (228) 688-5365

Standard Form 298 (Rev. 8-98)
Prescribed by ANSI Std. Z39.18

Validation Test Report for a Genetic Algorithm in the Glider Observation STrategies (GOST 1.0) Project: Sensitivity Studies.

1. Introduction

The Environmental Measurements Path Planner (EMPath) is a Genetic Algorithm (GA) software that has been developed for directing sampling platforms (such as autonomous ocean gliders) on preferential paths to achieve more effective coverage or transits in an area of interest (Heaney et al., 2007). Glider Observation Sampling Strategies (GOST) translates a glider sampling strategy into criteria for evaluating alternative glider paths through EMPath. In GOST 1.0 optimal paths are designed to target areas of large model forecast uncertainty; GOST 2.0 will expand mission criteria to include area coverage and searches to define relevant ocean features. By using environmental model data, EMPath evaluates alternative sets of glider instructions by determining the resulting glider motion subject to available descriptions of currents and other variables that will impact the glider's mobility. EMPath evaluates the resulting sets of glider trajectories relative to a cost function that quantifies the relative benefit expected from different sets of observations and identifies the most effective set. Observations from gliders directed according to the EMPath guidance will be more relevant for assimilation into the real-time models addressing the GOST-defined mission for the target area. Utilization of these tools for glider placement under GOST assists the Navy in optimizing the value of glider observations while reducing manpower requirements (Memorandum 3100; Memorandum 3140). Future goals of increasing the number of gliders in a Navy observation networks will only be manageable with such automation. Using the GA to do the background work of optimizing glider paths, particularly with the longer mission time frames encompassed by GOST 2.0, allows the operational center to adopt a proactive approach that maneuvers assets through changing ocean currents. This will insure that they are more effective in sustaining extended support for mission objectives.

EMPath interfaces with the Relocatable Circulation Prediction System (RELO) which has been operational since August, 2008 (Rowley, 2010). RELO has two major components: 1) the Navy Coupled Ocean Data Assimilation (NCODA) (Cummings, 2005) for data analysis and model initialization, and 2) the Navy Coastal Ocean Model (NCOM) (Barron et al., 2006; Martin et al, 2009) for the ocean dynamics prediction. The system also has the capability of performing ensemble runs initialized by the Ensemble Transform and forced by atmospheric fields perturbed by the space-time deformations method (Hong and Bishop, 2007; Coelho et al. 2010a).

This report will discuss two basic sets of experiments that have been conducted to evaluate the effect of EMPath in guiding gliders to the best location to provide feedback to an ocean model. The first set performs an Observation System Simulation Experiment (OSSEs) (Masutani et al., 2010) in the Okinawa Trough. In this approach one model simulation is designated to be the *true* ocean, often called the nature run, from which data can be extracted and assimilated in the other simulations. Another run is identified as the control, a run which employs the present standard

Manuscript approved June 13, 2012.

observing systems and assimilation capabilities. For these experiments, the inputs for the GA are derived from several criteria to test the impact of providing glider guidance from station and trajectory variability versus the forecast uncertainty as derived from an ocean model ensemble. The goal is to evaluate the skill and limits of each approach. The second set of experiments, the Maritime Rapid Environmental Assessment of 2010 (MREA10) is a true real time exercise with a full feedback cycle using model prediction to guide the glider and assimilating the collected data back into the model. Although not a Naval exercise, the MREA10 was used to exemplify the data flow challenges of a real-time Naval exercise similarly to the execution of such a system on Naval Oceanographic Office (NAVO) computational platforms.

2. Genetic Algorithm Background

The Environmental Measurements Path Planner, EMPath, (Heaney *et. al*, 2007) determines an optimal search plan for a network of inhomogeneous sampling platforms. The multi-objective cost function (CF) to be minimized is a linear combination of individual constituent cost functions (CCF). These CCF contain the oceanography, physics and Navy mission related information which the expert-user determines drive his update criterion. Current CCF are based upon model forecast uncertainty, ocean temporal-spatial variability and, if user interest merits, ocean acoustic sensitivity for ASW applications. The CF for a specific asset laydown strategy, $E(\vec{r})$, is the normalized, weighted sum of the user defined constituent cost functions. Constraints, such as these include boundary constraints, C_b, including bathymetry, operational area definition, and water space management. For multiple vehicle optimization, the distance-potential constraints, C_{dp} are used to keep multiple vehicles apart and are added to the user defined normalized sum. The CF is then expressed as:

$$E(\vec{r}) = \sum_{i=1}^{n} \frac{W_i C_i(\vec{r})}{\sigma(C_i)} + W_b C_b + W_{dp} C_{dp}(\vec{r})$$

where W_i are the user specified weighting functions and $\sigma(C_i)$ is the normalization term for each cost function. The normalization term is the rms value of a each sample cost function, such that, the large differences in magnitude of the multiple-cost functions can be accounted for, resulting in a non-dimensional CCF.

The genetic algorithm (GA) is a search technique for solving constrained large-dimensional non-linear optimization problems (Goldberg, 1989). The GA algorithm has been successfully applied to many of these problems, including for example geo-acoustic inversion in underwater acoustics (Gerstoft, 1994, Gerstoft and Gingras, 1996). The algorithm is loosely based on the process of natural selection in evolutionary biology. A gene is defined as a vector that uniquely determines a parameter of the search space, such as sensor platform deployment coordinates. Based upon the analogy of natural selection a population is generated from a random sampling of a particular gene pool, which spans the multi-dimensional search space. A population is a set of individuals, each having a set of genes specifying a unique measurement approach, which we refer to as the sensor laydown. For example, in a five-glider problem, each individual represents a different time/space transect pattern for five gliders. Beginning with an initial random sampling scheme (first generation), and iterating over generations, a gain over the cost function (or fitness) of each individual is computed. Using this information, fit individuals are selected and mated and a new generation of individuals is produced. Unfit individuals (those with poor fitness values) are not reproduced. A random crossover of parent genes generates the genes of the children. To reduce the probability of converging to a local cost-function maximum, a small fraction of random mutations of individual genes are permitted for each generation. Reproduction and fitness testing occurs until an exit criterion is met. Example exit criteria are a minimum percentage change in the fitness function, or a maximum number of generations.

EMPath includes a simple kinematic model for each platform, moving within a forecast ocean velocity field. The velocity of the platform is added linearly to the forecast ocean current vector as a function of time. The inclusion of ocean current in the generation of the path sampling vector constrains the solution space to searches that are achievable – to within the accuracy of the ocean forecast velocity field.

The primary purpose of the morphology figure is to provide a display for the user with a level of confidence that the GA has indeed guided the network to regions where the constituent cost functions are large. The morphology computation is an estimate of the integration of the cost function which the Genetic Algorithm is using to optimize sensor locations. To estimate the shape of the multi-dimensional cost function (the morphology), a glider is positioned at lat/lon grid in the NCOM forecast ocean field. The cost function is estimated for a glider trajectory due north, due east, due south and due west for as many hours as specified by the user (morph_hours). The score for the 4 trajectories are averaged into the morphology estimate for that location. A short computation time leads to higher resolution figures, with less horizontal averaging, but underestimates the temporal dynamics of the 4D cost function. A longer time morphology computation, smoothes the spatial scales, but includes the CCF at later times.

2.1 Targeting Observations Using Ensembles

The problem of adapting the best location for deploying mobile observation platforms in a dynamic environment is often called the adaptive sampling or targeting observation problem. The importance of this topic has been heightened in oceanic applications by the advent of Underwater Automated Vehicles (UAVs). Planning the missions of these platforms includes updating reference way-points on regular schedules such that one must solve the adaptive sampling problem before some critical decision time. For this purpose, the Target Observations Using Forecast Uncertainties (TOFU) (Coelho, 2010b) system uses a method applied by Majumdar et al. (2002) to adaptive sampling in atmospheric modeling applications. This technique uses the ensemble forecast (Bishop et al., 2001) and rapid low rank solutions of the Kalman filter equations to solve the targeting observation problem. The enabling technique Ensemble Transform Kalman Filter (ETKF) allows for a mapping of the error covariance through time and space. This is based on the assumption that the analysis error covariance at the observation time can be estimated by evaluating the reduction for each feasible grid point of the ensemble domain, taken as a single profile measurement, through a range of selected depths (for the present example 0 to 1000m to reproduce a glider profile observation).

The first step of this method is to identify the areas of interest inside the simulation domain hereby referred to as the target box. A forecast time called a verification or target time is one in which the adaptive supplemental observations taken at an earlier observation time will produce a maximum effect defined by a fitness computed over the cost function. For this TOFU version all these parameters are to be introduced using a Graphical User Interface (GUI). The cost function to be minimized is derived from to the ensemble forecast variance of the temperature and salinity and the parameters computed by the IAMPS system (Zingarelli and Fabre, 2009).

2.2 Ocean Variability Cost Functions

There are operational situations where due to limited computational resources an ensemble forecast is not available. For these situations we estimate regions of model uncertainty using a central forecast using a default program, datacx (Heaney et al, 2012.) It is assumed that regions of stronger dynamic oceanography will be correlated with regions of model uncertainty. Certainly, one can expect the converse is true: regions where there is little spatial or temporal variability are regions where the model uncertainty is expected to be small(assuming initial model bias had been removed at initialization). To this end, we define a temporal cost function as:

$$C_{Temporal}(\vec{r}) = \left\langle \left(T\left(x, y, z_{ref}, t\right) - \overline{T} \right)^2 \right\rangle^{1/2}$$

$$\left\langle \overline{T}\left(x, y, z_{ref}\right) = \left\langle T\left(x, y, z_{ref}, t\right) \right\rangle \ \right\rangle$$

respectively, where the temporal *rms* and the averages are taken at each location in space (for a specified z_{ref}). The fitness over these functions is computed by line integration over the possible glider tracks $\overrightarrow{(r)}$.

Other sets of functions aimed to look a the combined space-time variability are designed directly from the state variables (or other fields of interest). On these the fitness is computed by differentiation over the trajectories such that those capturing fronts will show a larger skill. (The EMPath User's Manual (Heaney et al, 2012) has a more complete explanation of appropriate EMPath and datacx usage and parameters.)

3. Observation System Simulation Experiments (OSSE's) in the Okinawa Trough

The Okinawa Trough region has been used as a testbed for our theoretical setting (Fig,1). From August to November 2007 the area was surveyed extensively and used to populate the Naval Research Laboratory - Stennis Space Center (NRLSSC) data server including databases restricted to the Department of Defense (DoD) obtained by NAVO, as well as public data sets. The RELO model domain configuration is similar to the one applied to assess the acoustic performances predictions (Rowley, 2010, Rowley et al., 2009, Coelho et al., 2010b). After an initial spin up, the experiments were concentrated in the period Oct 15-Nov 1, 2007. The operational area (where gliders are allowed to sample) spanned from 121-127ºE and from 20-

27^{o}N and the target area (where forecast skill is expected to be improved) ranged from 123-124^{o}E and 23-24^{o}N. Six gliders were assumed over the operational area, sampling to a maximum glider depth of 1000m. Each EMPath cycle allowed for 500 generations and 100 individuals and 20 repetitions. From these executions the EMPath provided a set of hourly latitude and longitude positions for each glider over a 48-hour period.

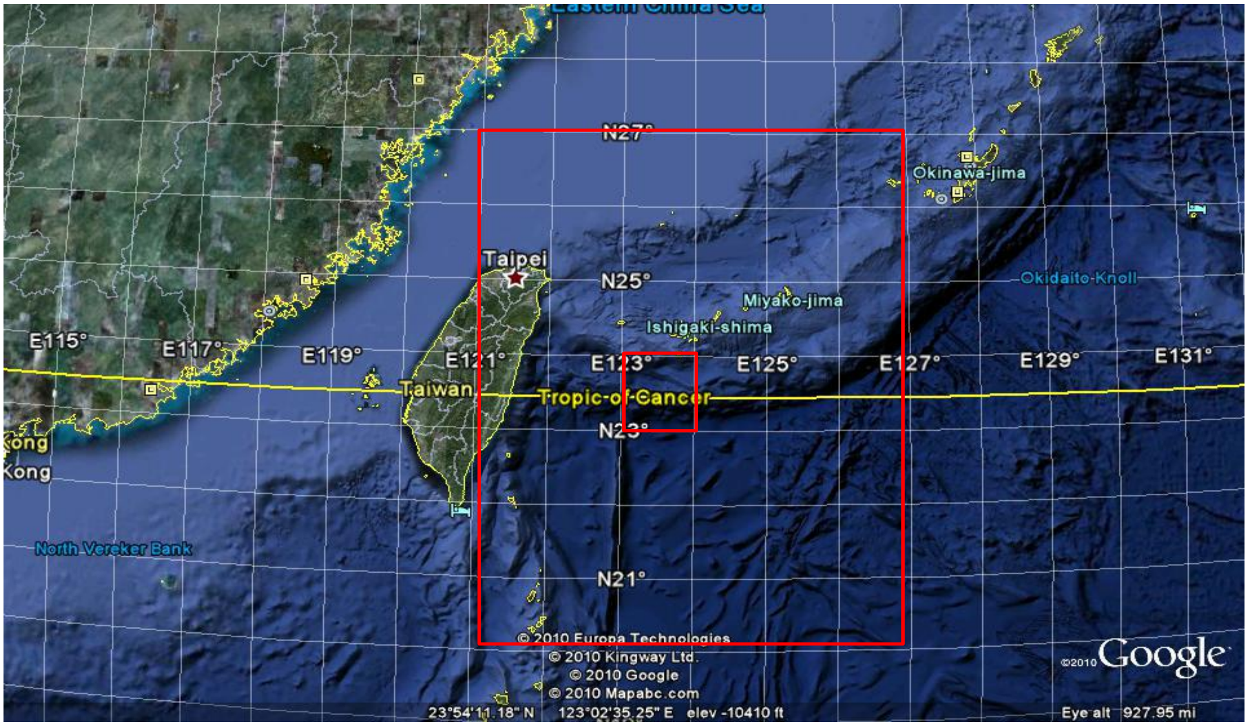

Fig. 1 The experimental or operational area(20-27^{o}N,121-127^{o}E) is shown in the outer box and the target area (23-24^{o}N,123-124^{o}E) in the inner box.

3.1 Explanation of Numerical Experiments

A RELO run assimilating all the available data over a 12hr NCODA cycle is designated the **Nature Run** (natrun) or truth (Fig. 2). Several variations of this RELO run were used in this VTR. Unless otherwise specified all the simulations are forced by the Coupled Ocean/Atmosphere Mesoscale Prediction System (COAMPS_wpac 2) winds (Hodur, 1997) and heat fluxes from 0.5^{o} Navy Operational Global Atmospheric Prediction System (NOGAPS) (Hogan and Rosmond, 1991). Several criteria, simulating different possible applications in a real-time scenario were applied to the NCOM fields for providing CCF to the EMPath algorithm.(Fig. 3). When data assimilation is included, the NCOM runs provided a 48 hr forecast. These CCF and the forecasted ocean currents were used to provide hourly waypoints for the glider trajectories, updated every 48 hours. Note that US Navy guidance is given with 12 hr separated waypoints, but for this experiment we assume the gliders to follow recommended trajectories. From these trajectories, simulated glider observations were then produced by sampling the natrun at each glider's location and times. Our goal is to verify that the assimilation of the glider profiles will improve the model performance.

The comma separated variable file provided by EMPath (Heaney et al, 2012) for glider guidance are used as the input for a NCOM post-processing routine to extract simulated profiles of temperature and salinity from the nature run's output. For a temporal interpolation, the simulated profiles are at every hour and every following hour (one hour is the time interval of the NCOM output files) .

The different cases are:

- **Control Run (contrun)** is the benchmark case. It includes data assimilation of all available data from the NCODA directories, but no profiles from gliders or from NCODA.

- **Case A** which will be referred to as **ok_free is** a free run (ie no data assimilation). The model is forced by atmospheric fields and restated by the previous day simulations.

The previous two cases are variations in model spinup and initial conditions. The following cases refer to different manipulations of the model outputs to make cost functions.

- **Case B is** the run with 32 ensemble members. From the ensemble mean and variability, TOFU created the NetCDF file that serves as input to EMPath. The TOFU GUI creates a summary map fromf RELO NCOM acoustic and tactical ensemble members which is referred to as an ETATM file, which also includes a set of 22 CCF in temperature (T), Sonic Layer Depth (SLD), and below layer gradient (BLG). The summary maps identify relative impacts of each grid point if sampled independently in reducing the forecast error over the target area.

- **Case C** uses a cost function based on the error between the RELO forecast and the natrun. An absolute temperature difference file is generated between the natrun and the NCOM forecast over the 48 hours of fields:

  $$\text{Error} = |\, T(x,y,z,t)_{\text{natrun}} - T(x,y,z,t,)_{\text{NCOM forecast}} \,|.$$

  These differences are normalized over the forecast period and fed into a datacx pre-conditioner (Heaney et al, 2012). The NCODA processing in the simulations runs daily using this absolute temperature differences instead of the usual error between analysis and forecast (Rowley, 2010). This represents a perfect cost function which though not possible operationally, could be extrapolated to areas where there are known simulation errors.

- **Case D** uses the RELO forecast temperature and salinity variability to compute the cost function. This is the backup for operational areas to received information on ocean dynamics when not running ensembles. In some areas of interest, the executing of ensembles is not always feasible due to computer resource limitations. The datacx pre-conditioner reads the files over the forecast period and normalizes the variability to calculate a CCF. The NCODA is based on the error between analysis and forecast fields.

- **Case E** is a lawnmower case which would closely resemble an array deployment of gliders. Gliders are initialized to a starting position and given a bearing to go from west to east and back. EMPath was only used as a kinematic solver to confirm the feasibility of straight line glider paths in the presence of the forecast ocean model.

For each Case, we have conducted parallel simulations as summarized in Table1:

- **Case B-E** henceforth as referred as to as the standard set. The models are initialized by the contrun and include assimilation of all data. Gliders are directed by EMPath. We also have a twin experiment, **CaseBr**, to verify the impact of different correlation length scales in the d**ata as**similation and model performances, as it will be discussed at a later section

- **Case Bf-Ef**: models are initialized by the free run and during the two week comparison time include assimilation of all data. The purpose of the free running initial conditions following the free running startup was to compare an addition of these capabilities to a more simple simulation. The simulated profiles from the natrun over the glider paths were not recalculated. The gliders' travel paths are from standard case (ie EMPath was not re-executed). These simulations are henceforth as referred as to ICfree.

- **Case Bp-Ep**: models are initialized by the contrun and assimilate only the profiles (no surface data was assimialted) with the goal of isolating the gliders' impact. Even though other profile data are present, the glider data will still provide the bulk of the assimilation depending on the configuration of gliders. As in the previous alteration, EMPath was not rerun. This simulations are henceforth referred as to as profDA.

Table 1: Glider treatment vs. pre-processing

	Initial Condition/Data Assimilation		
Glider Treatment	-IC/contrun -all available data	-IC free run -all available data	- IC contrun -/glider profiles only/no surface data
Ensemble spread	Case B	Case Bf	Case Bp
Known Forecast Error	Case C	Case Cf	Case Cp
NCOM Forecast	Case D	Case Df	Case Dp
Lawnmower	Case E	Case Ef	Case Ep
No assimilation		ok_free	
No gliders/all other available surface data	contrun		
No gliders/all other available surface and profile data	natrun		

The horizontal interpolation of glider data in the form of a profile is bi- linearly interpolated to the nearest point to map these data onto the model grid. The vertical interpolation algorithm is done using a Piecewise Cubic Hermite Interpolating Polynomial (Fritsch et al. 1980, Kahaner et al. 1988) that preserves the profile shape, retains the monotonicity and matches the maximum/minimum values at the points of the original field. The latter properties may have some effect on our evaluation as it will be discussed in a following section. A subsequent script shapes interpolated profiles in a descending-ascending triangular path at four minutes intervals. This is accomplished with a linear vertical interpolation between each hourly waypoint and the waypoint for the following hour to simulate the glider movement. Therefore the whole procedure requires a great amount of interpolation that definitely may compromise our evaluation.

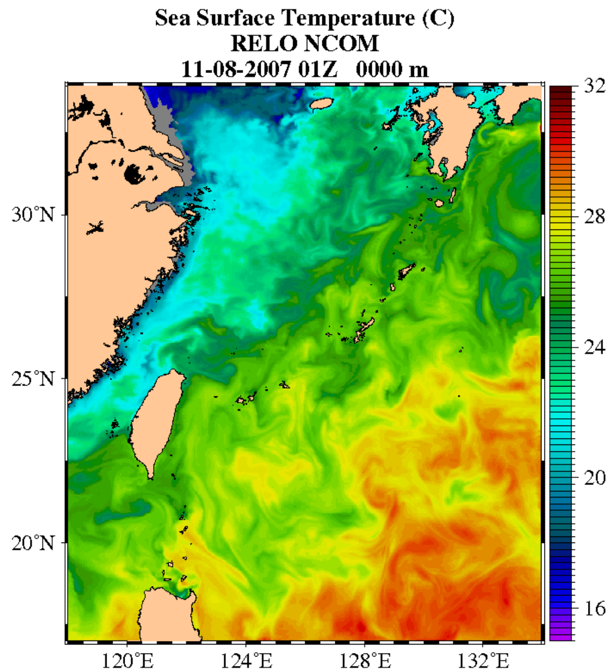

Fig. 2 A snapshot of the Nature run or "truth"

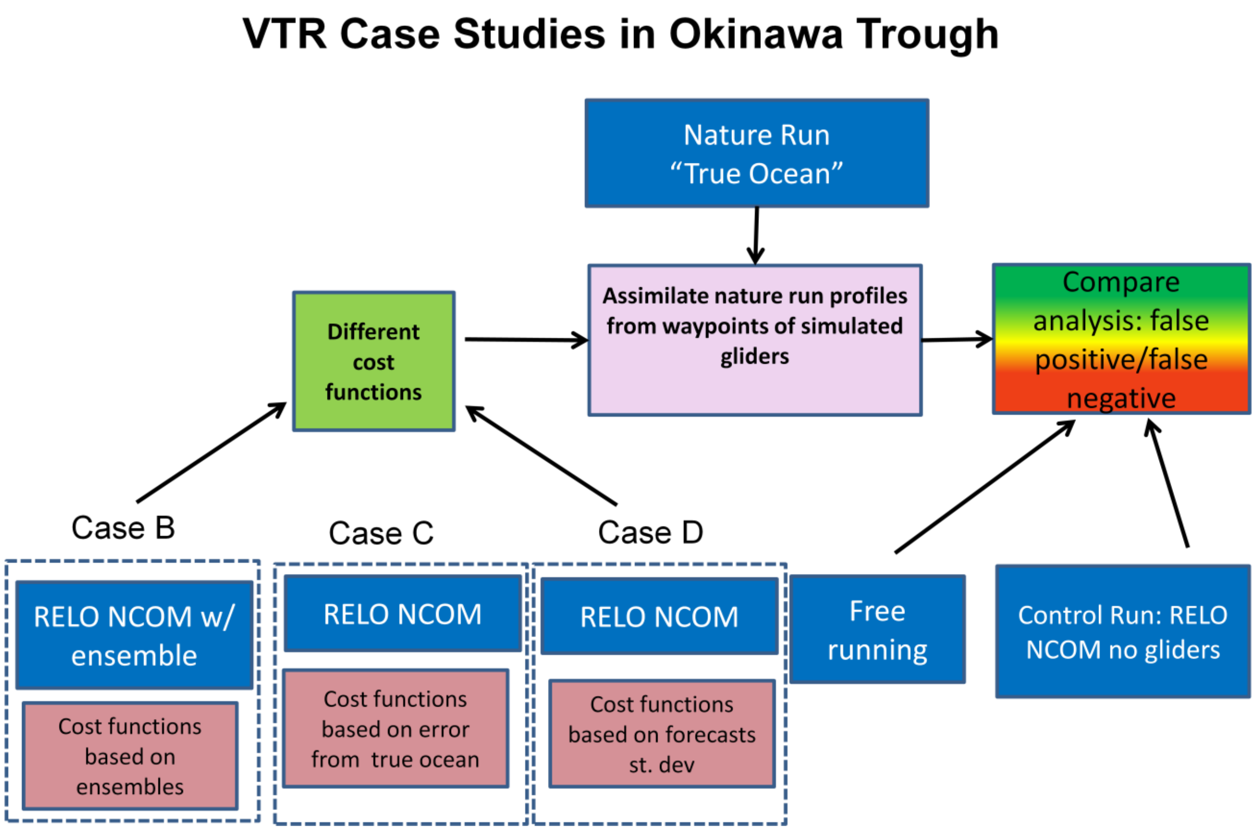

Fig. 3 The case studies in the Okinawa Trough area

Figure 4 is an example of differ EMPath best waypoint solutions to illustrate a typical glider guidance delivery. The glider paths are placed over the morphology All cases are best solutions of the highest level of confidence of large CF for 2 November 2007 and are plotted on different scales. This illustrates the different emphasis of the various approaches over the operational area.

The high impact area is indicated by the red in the morphology. For Case B, the TOFU provides a clear area of high morphology. The case B gliders can travel outside of the target area, but will remain in the operational area. Figure 4b illustrates Case C glider behavior. Case C, while having more information available than is realistic, looks for known maxima in the operational area. The gliders movement however, is severely limited as seen by the almost nonexistent tracks. Case D's color scale (Figure 4c) illustrates that it does not determine obvious maxima over the operational area, but it does produce a robust coverage. Case E as shown in Figure 4d, allows the gliders to attempt ideal lawnmower paths back and forth over the operational area. The gliders show a slow drift but try to follow a man-in-the-loop determined path.

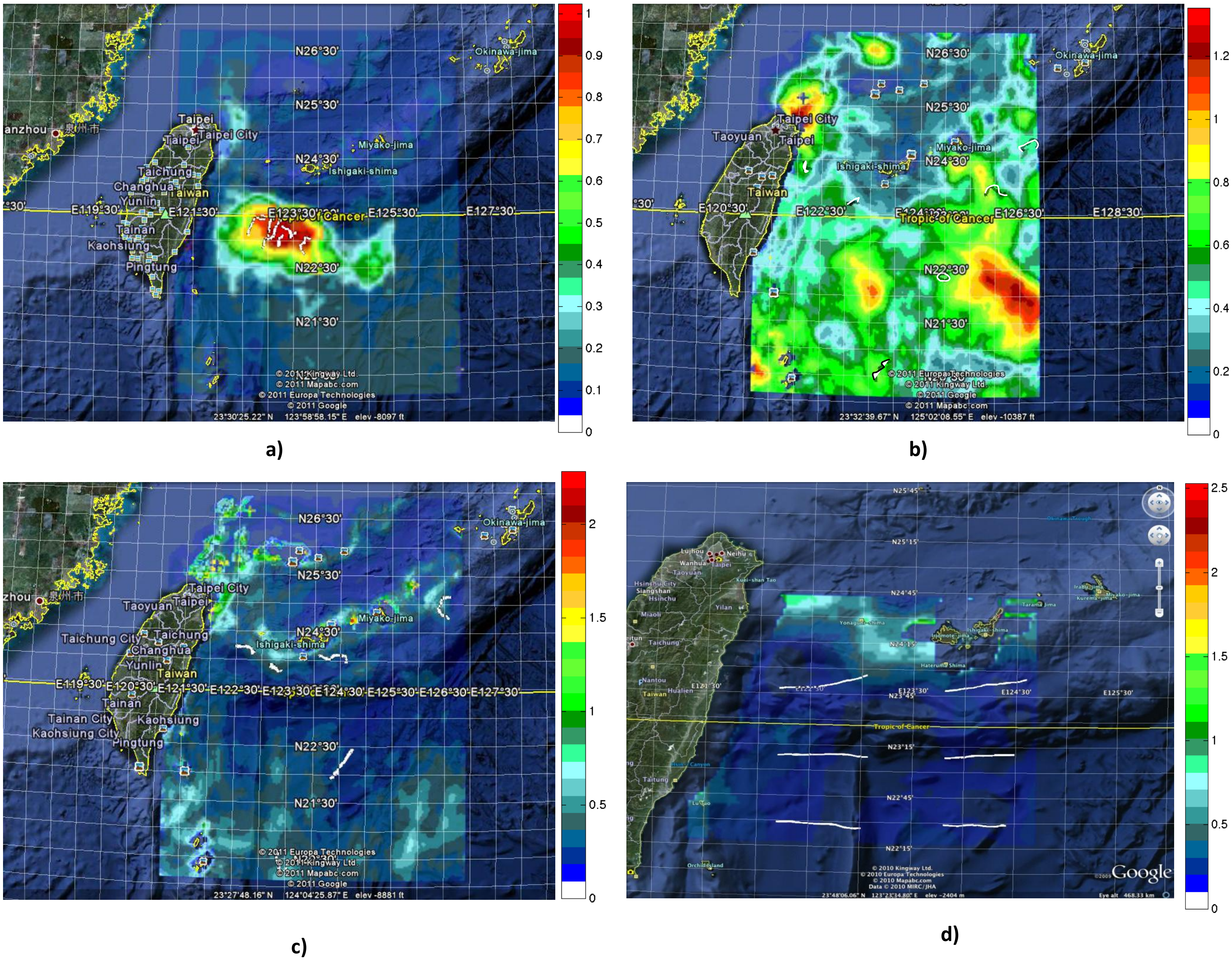

Fig. 4 Examples of glider paths from Case B(a), Case C (b), Case D (c) and Case E(d) for 2 November 2007.

3.2 Results

Our goal was to evaluate how the assimilation of the glider simulated profiles affect the prediction of the acoustic properties. Therefore, our analysis was focused on the representation of the SLD, that corresponds to a key variable determining the skill in trapping sound waves in the upper ocean (Helber et al, 2010). Fig. 5 illustrates a day, 1 November 2007, in which the natrun has a preponderance of low SLD and the free running case has mostly higher, highlighting an extreme disagreement needing a correction. The obvious red bias in the free running case (b); as opposed to the more blue areas in the nature run (a), illustrate areas where glider improvements might be easily visible. This particular date is chosen for comparison because the error was obvious to the naked eye.

The control run case and standard glider cases all show improvement over the free running (Fig. 5c-Fig. 5g). The plots of the free running initial conditions show the glider impacts more clearly (Fig. 5h – Fig.5k). Case Ef appears to have the most overall impact due to coverage. With glider profiles only (Fig. 5l – Fig.5o), the data assimilations of the surface fields does not occur. This makes it possible to see the slicing of the gliders into the red areas with the correct "blue" data. Realistically, there would usually be other NCODA data available. The glider only experiments were an additional check to observe the glider data impact. Fig. 5l-5o show the slicing of the gliders to introduce the blue (lower SLD) into the formerly red area.

These plots were created to initially assess the impact of any data over a free running case. All of the assimilated cases make some improvement over the free running case.

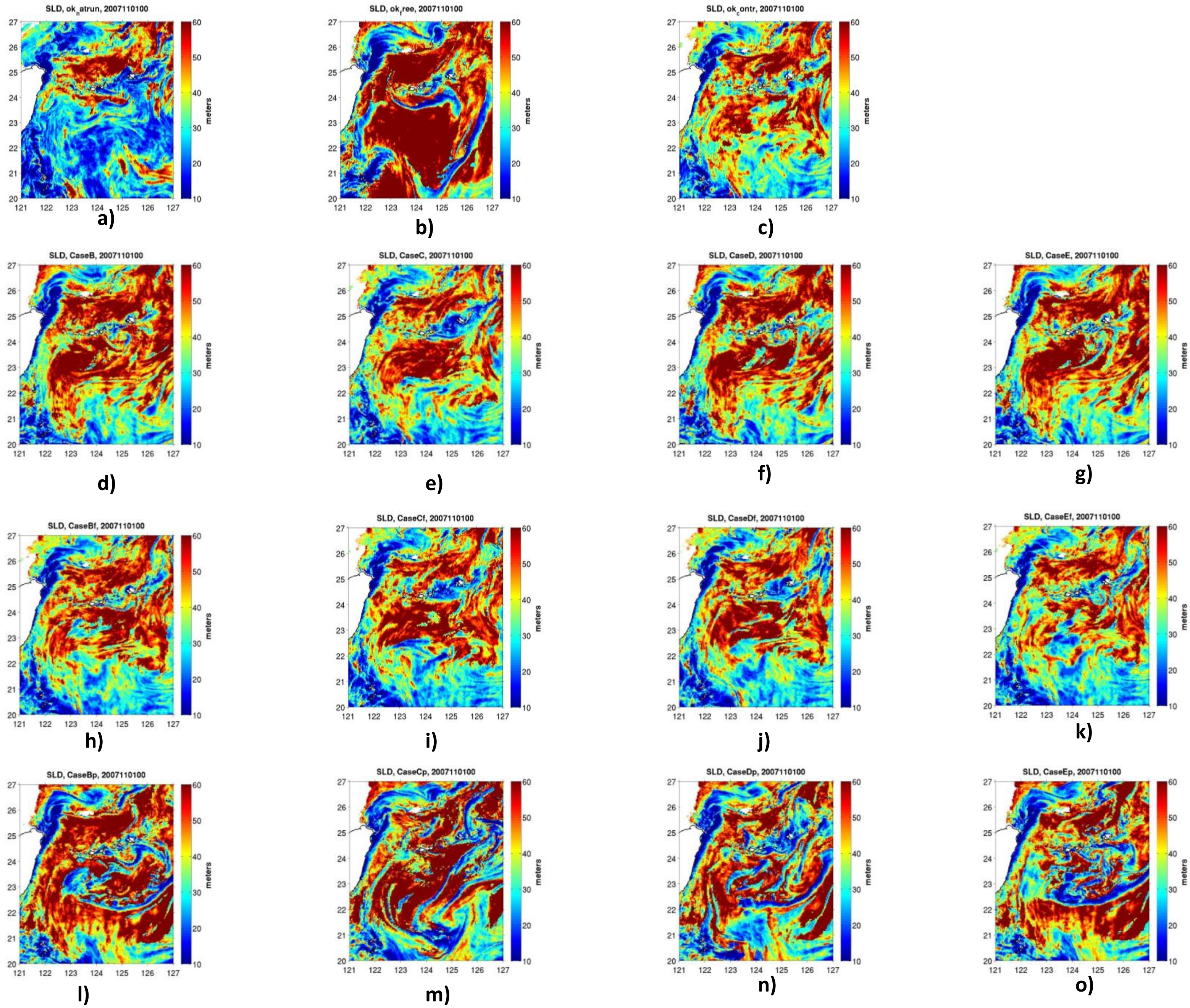

Fig. 5 Sonic Layer Depth plots for 1 November 2007.

Fig 6 illustrates the mean and RMS error of SLD between the different cases and the natrun (true ocean) as a function of time over the target area for the standard cases.   The mean and RMS were calculated over the target area. The results didn't provide the expected improvement and no case appeared manifest as the 'best' of the approaches. We have therefore questioned the OSSE configuration. From our analysis, two major limitations have emerged: 1) the true and simulated oceans were too similar for an effective application of NCODA, and 2) the extensive interpolation applied for extracting the glider profiles.

One of the major parameter in NCODA is the specification of the correlation length scale (ie the radius of influence for the assimilated profile). In our cases, since no substantial differences were in the true and assimilated ocean, the correlation scale deteriorated (rather than improving) the solution in the proximity of the profiles. This is most likely due to interpolation and introduction in various forms to NCODA. To verify the validity of this assumption, Case B was re-run with a smaller (and unrealistic) correlation length scale (henceforth as referred as to as CaseBr). As Fig 6 indicates the error is sensibly reduced.   The horizontal and vertical interpolation applied to extract the simulated glider profiles has also a major impact. As previously discussed, the vertical interpolation preserves the maximum and minimum values at the original depths. Therefore, the thermocline depth, already poorly represented by the NetCDF coarse z-levels (ie the standard Generalized Digital Environmental Model (GDEM) 72 levels) was conserved in the interpolated profiles and small variations in the vertical field may have lead to large difference in the SLD computations.

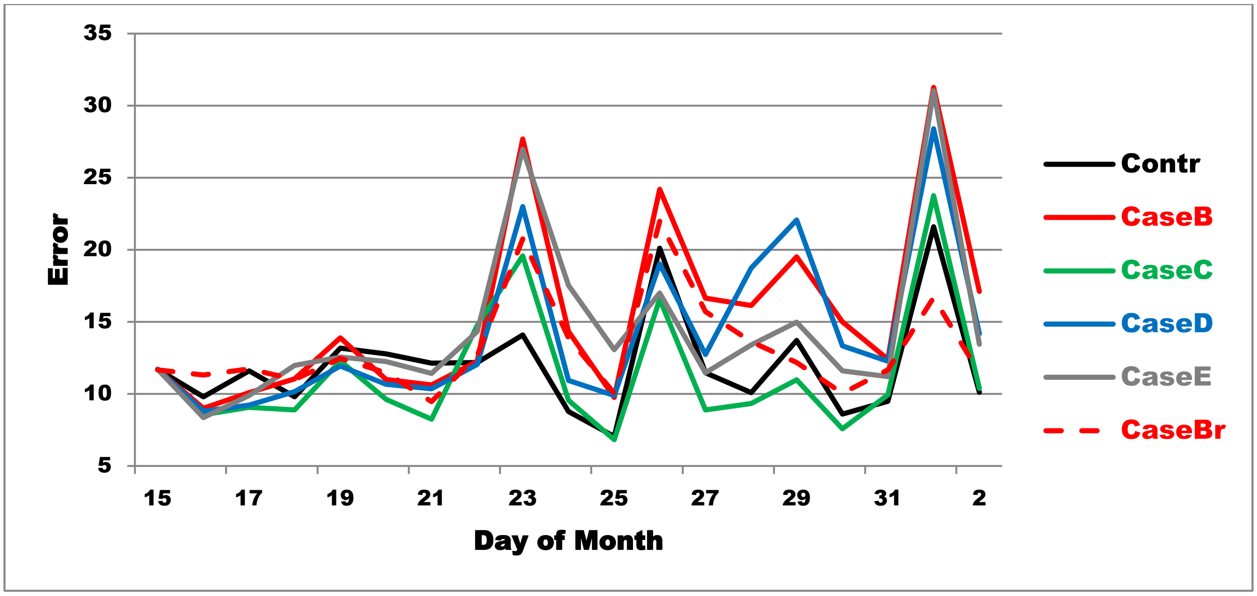

a)

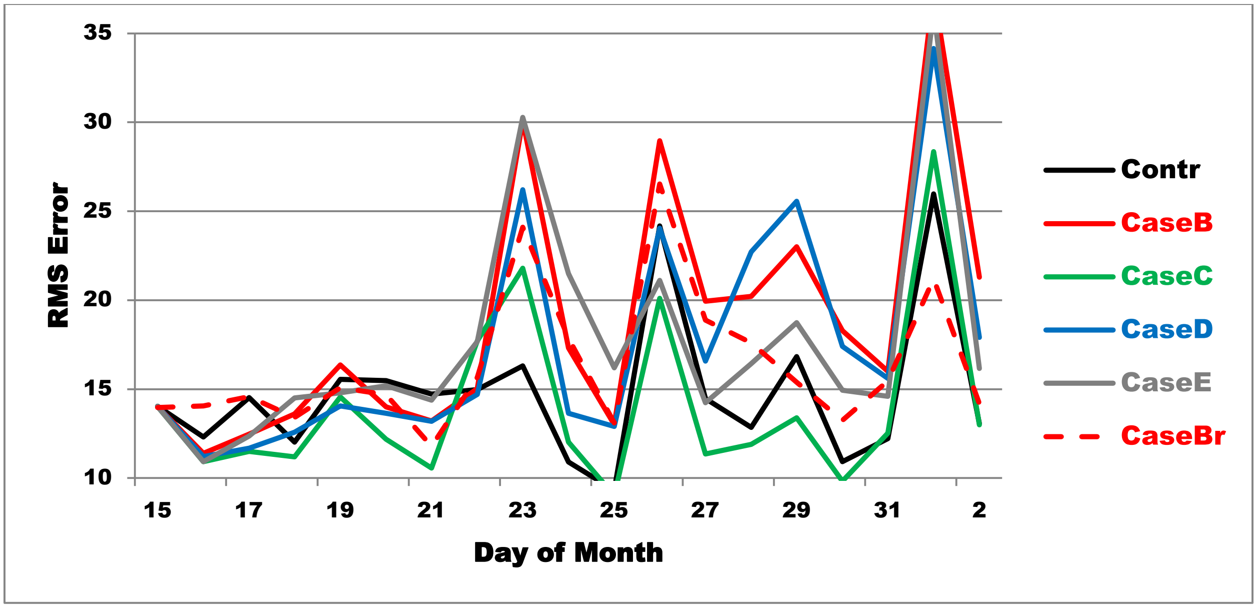

b)

Fig. 6 The mean (a) and RMS (b) error over the target area as function of time for standard cases.

Fig. 7 presents the SLD error time series for the ICfree cases. The glider cases make positive impact from the beginning of the simulation period over the control run. As with the standard cases, no one case appears to be clearly best, though Case B does well overall. From these calculations Case B and Case D would do as well as the man in the loop lawnmower type case.

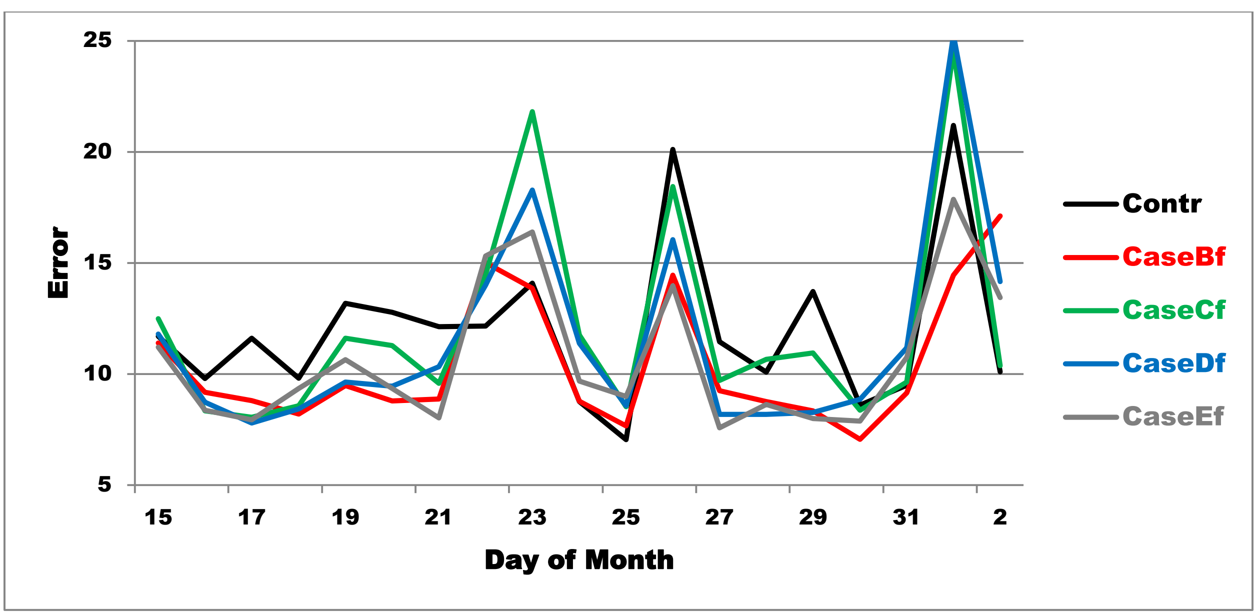

a)

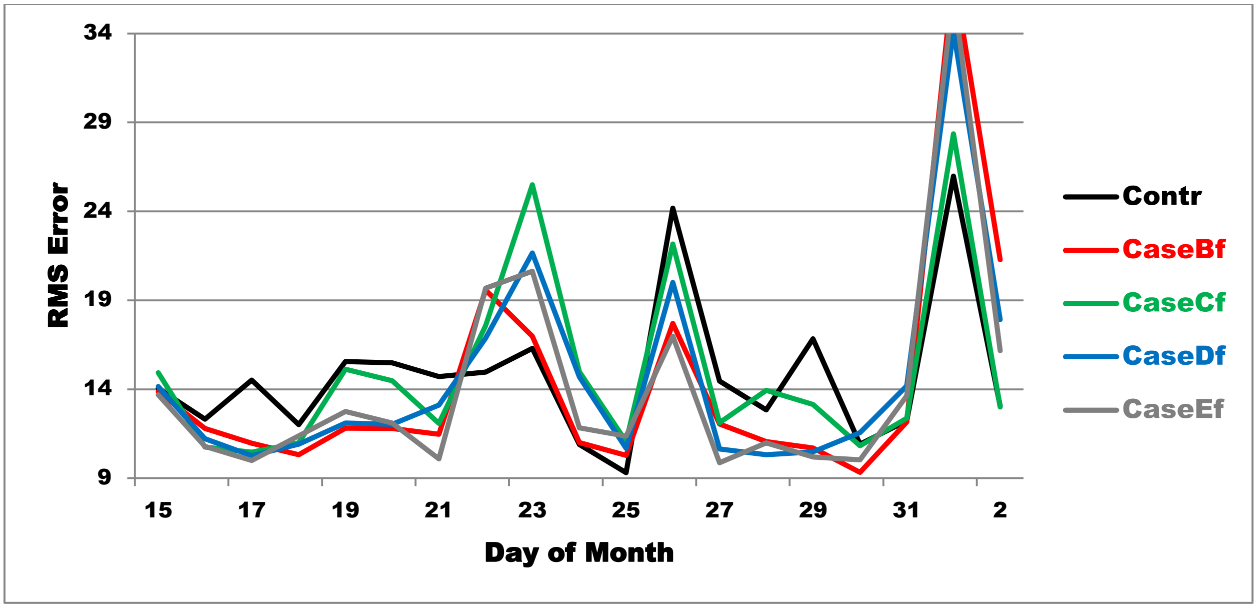

b)

Fig. 7 The mean (a) and RMS (b) error over the target area as function of time for free running initial condition (ICfree) cases.

Fig. 8 shows the ProfDA SLD error comparisons. The control run as expected would have the lowest errors, resulting from the additional data. Case Cp clearly has the highest error. This may be the result of restrictions on glider movement to high error areas, as was seen in Fig, 4b. Case Bp has a very low error overall which shows the success of the adaptive sampling as if focuses on the target area and the gliders cooperate.

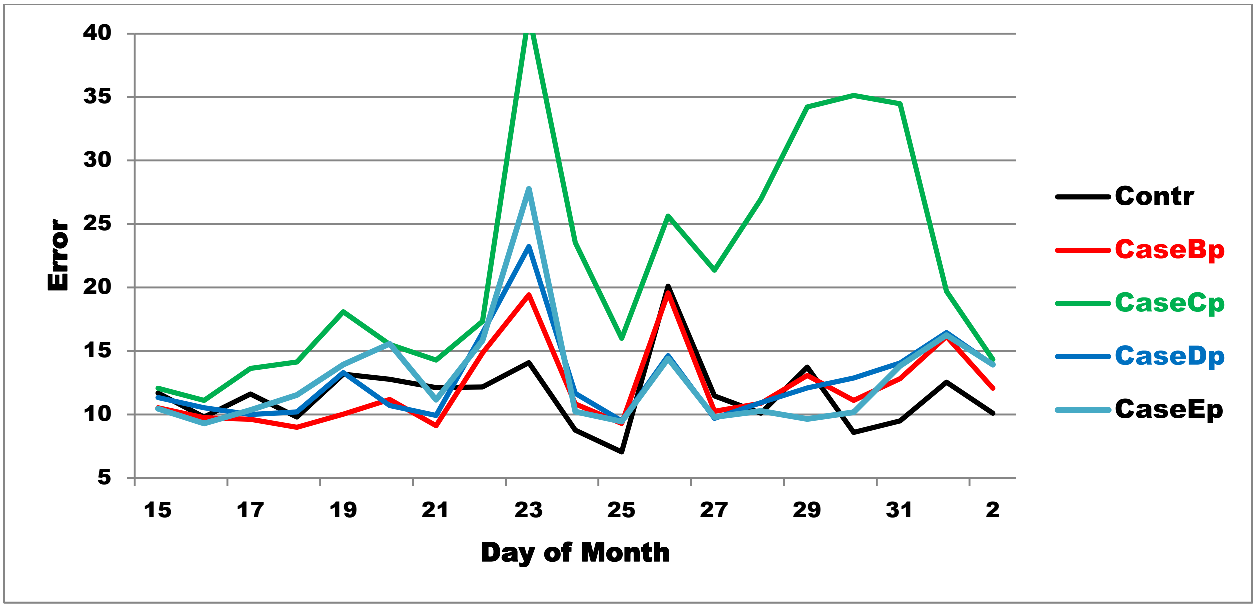

a)

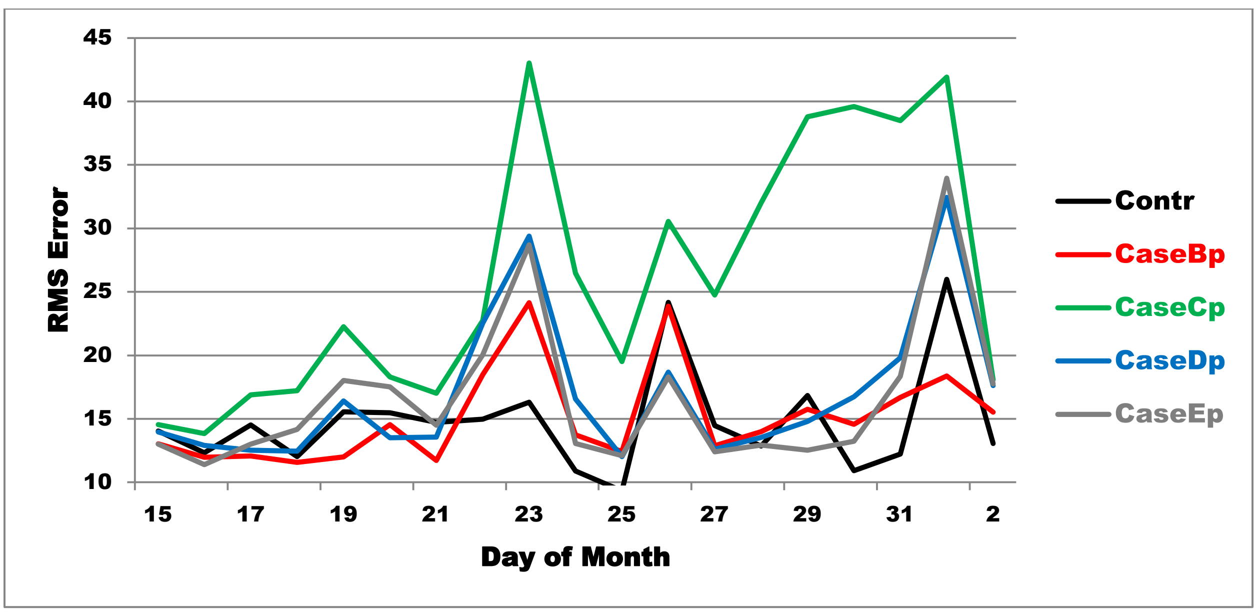

b)

Fig. 8 The mean (a) and RMS (b) error over the target area as function of time for glider profile data (ProfDA) assimilation cases.

We have also investigated the effect of the procedures on the detection skill and prediction of surface ducting by trapping sound at frequencies of 600Hz and higher.. An analysis was done using Matlab routines created at NRLSSC by Robert Helber to calculate the cutoff frequency (COF) (Helber, 2010Assigning a reference frequency of 600 Hz, comparisons were made between the COF of the natural run and the COF of the each case. If the nature run's COF was greater than the 600Hz, and the case study's was less, the case study had a false positive indicated by red. A false negative (yellow) occurred when the nature run predicted trapping and the case study did not.. A true positive, indicated by green, occurs when both experiments predicted trapping at less than 600Hz; and conversely a true negative (white) when both the case study and the nature run predict no trapping (Table 2). Fig. 9 depicts an example of stop-light plot over the target area.

Table 2 COF color scheme

	Model < 600Hz	Model >600hz
True < 600Hz	**Green true positive**	**Yellow false negative**
True >600Hz	**Red false positive**	**Blue or white true negative**

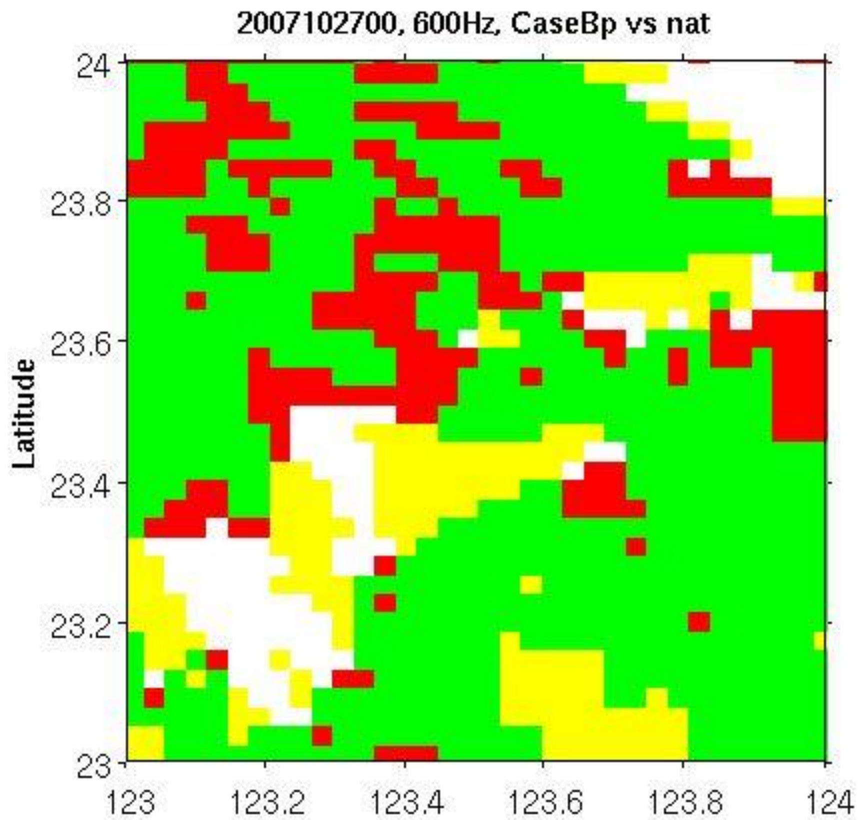

Fig. 9 An example of an SLD comparison between an experiment and the natural run; where red is false positive, yellow is false negative, green is true positive, and white is true negative.

Initially, the comparisons were made at analysis time 00. The investigation of behavior at 00 for the OSSE's illustrated the effects of gliders in an area over time influencing model analyses over many days. While the stoplight plots may present a spatial indication of false vs. true predictions, they do not allow us to quantify the impact of the glider data. Counts were added to the Matlab program and the results organized in histograms representing time 00Z (Fig. 10a-f).

Whereas red and yellow are incorrect (false) results, and blue and green are correct (true) (Table 2), the red and green are the most obvious in the histogram plots. As we step through the two week simulation period it is obvious that the results are not consistent throughout. The free running case (Fig. 10a) develops some predominantly green (true) results around October 20, 2007 and it continues to improve toward the end of the simulation which is unexpected.

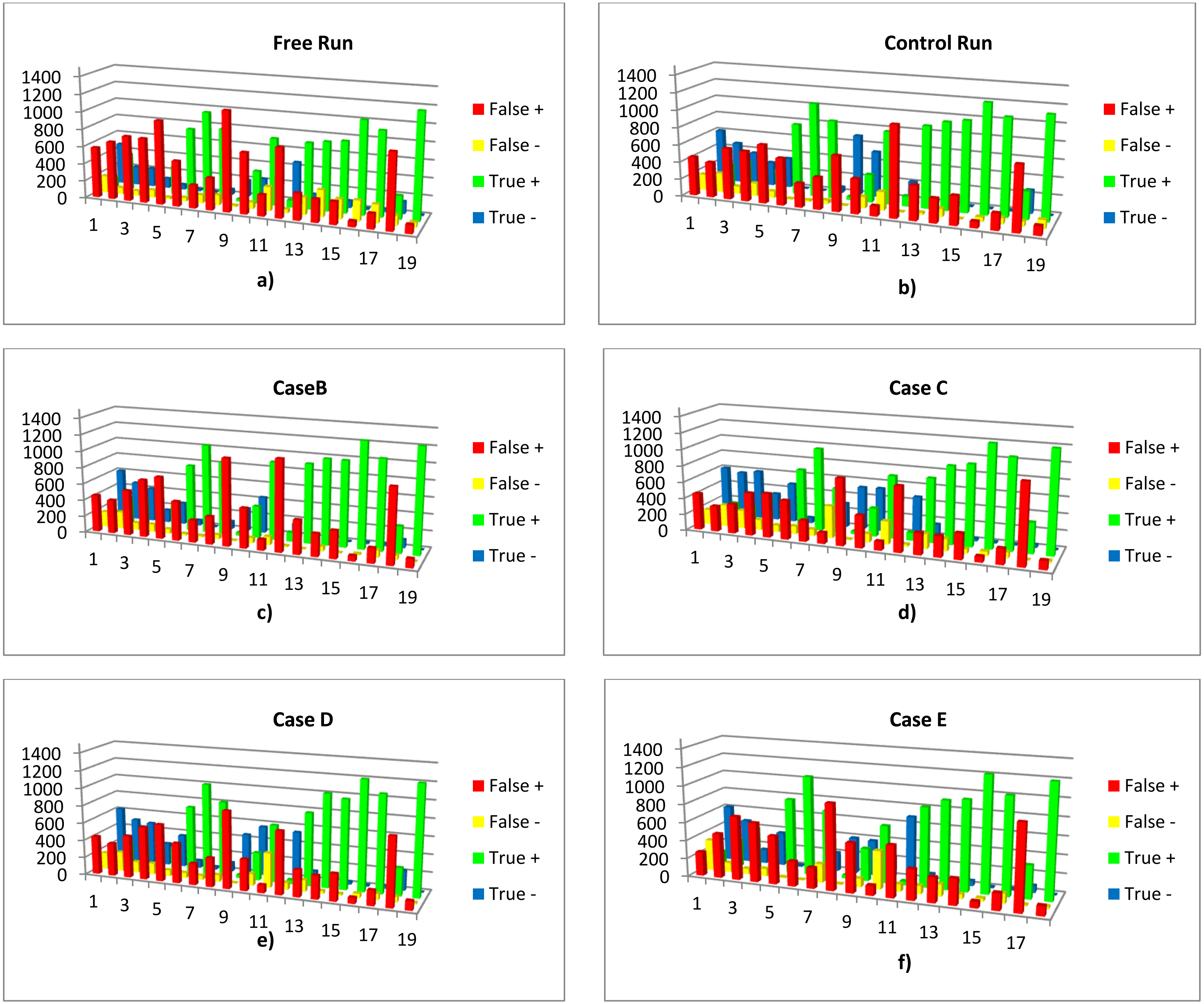

Fig. 10 A histogram to quantify the true vs. false variations along the nineteen days of the comparisons.

In Fig.10, the control run case shows some obvious blue and green results peeking out from behind the incorrect red bars which are decreasing from their values in the free run. The data assimilation makes a noticeable improvement for all cases on the first day.

Case C, (Fig. 10d) where the actual errors are actually known shows more improvement than Case B at day one, as expected, due to the knowledge of exact error. In Case D, (Fig 10e), the results are still favorable. Toward the end of the two week period, the true representation occurs more often than the false one. The Case E (man in the loop lawnmower), while showing some superiority towards the end of the 19 days, is not significantly better. (Fig. 10f) This suggests that assuming the gliders spaced at approximately equal distance and continues coverage would not be more beneficial than a genetic algorithm to zoom in onto problem areas.

The other sets of simulations ProfDA (Case Bp-Ep) and ICfree, (Bf-Ef) have similar behavior.

To further quantify the COF true vs. false comparisons, the green and blue (true) values, and the yellow and red (false) values, respectively, were averaged over the 19 day simulation period.. A straight subtraction of true minus false gives an indication of correct minus incorrect values (the optimal scenario would have zero incorrect values).

Fig. 11 illustrates the difference calculation of true and false assessments over the length of the run. The y-axis is the number of (true- false) points The highest values indicate the most correct. A negative value indicates more incorrect than correct values. The x-axis is the day of the model run from 15 October 2007 through 2 November 2007. The upward trend of the graph demonstrates the improvement over the two week simulation

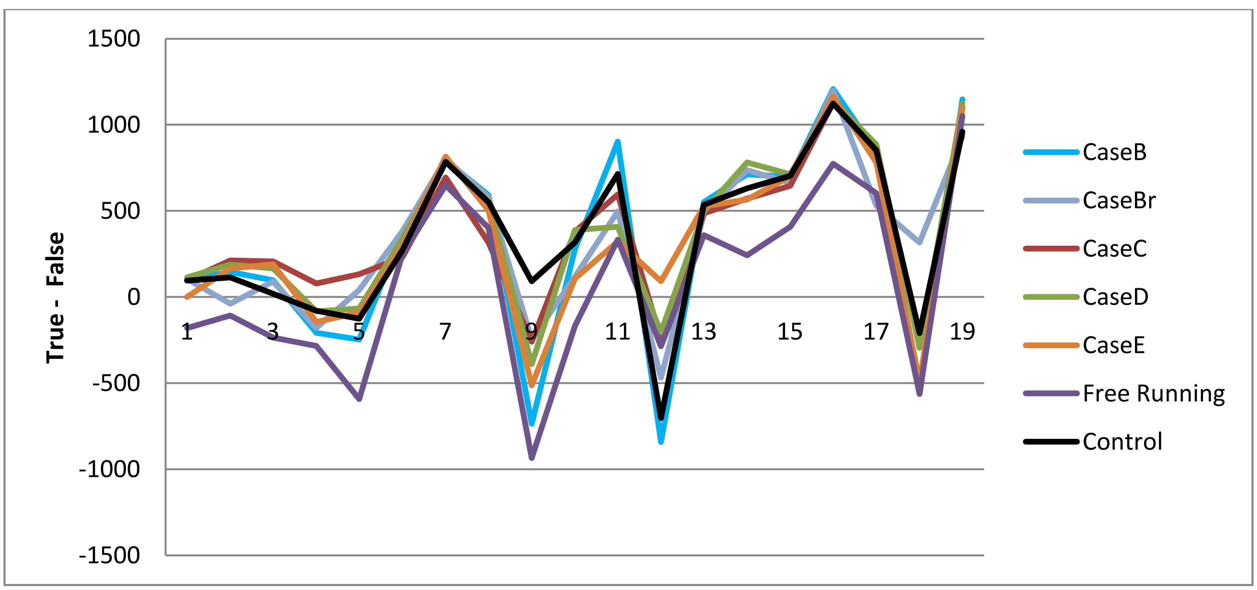

Fig.11 A running calculation of the difference between true and false calculations of cutoff frequency for the original OSSE's in the target area.

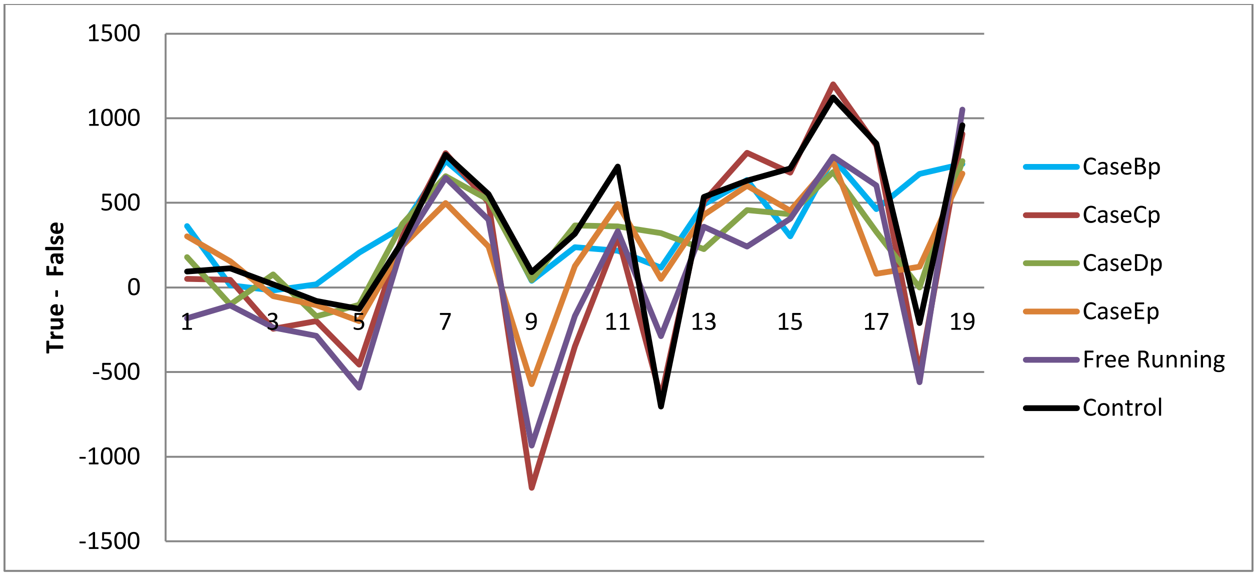

Fig.12 A running calculation of the difference between true and false calculations of cutoff frequency for the glider profile OSSE's in the target area.

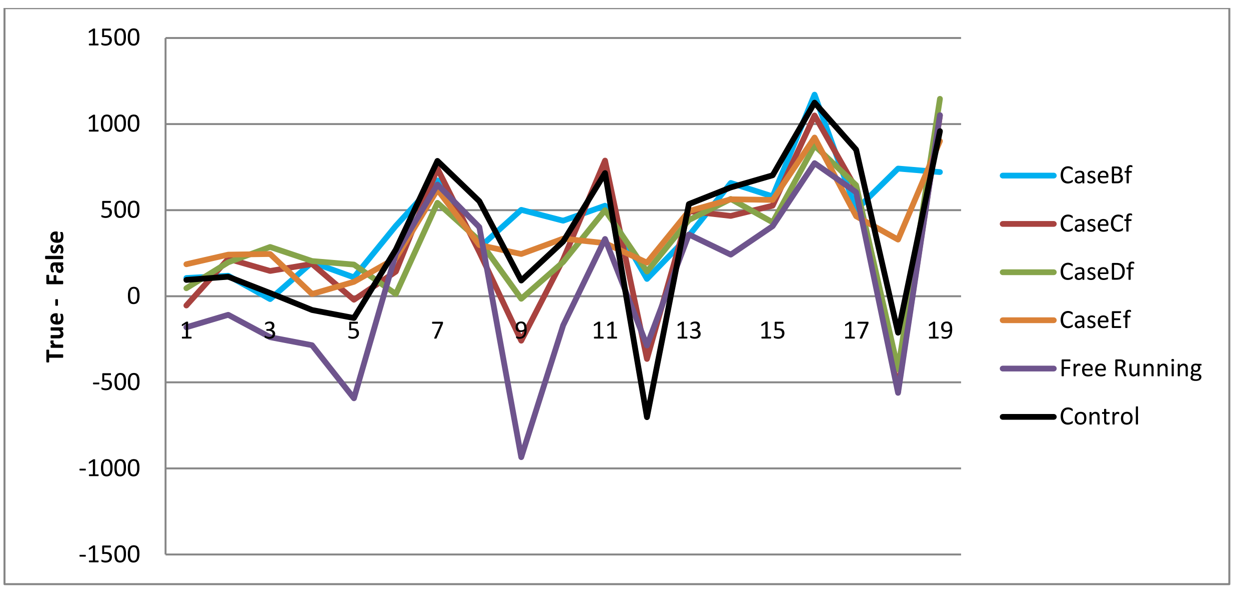

Fig.13 A running calculation of the difference between true and false calculations of cutoff frequency for the glider profile OSSE's in the target area.

Table 4 presents a calculation of the mean of the differences of the initial runs over the two week period. The percentage correct are calculated with a simple formula:

$$\frac{\#true - \# false}{\#true + \#false} \times 100$$

The largest positive numbers indicate that the cutoff frequency is more correct when compared with "truth." Case D is the winner in this set, which is interesting as the calculation is only done over the target area. Therefore, Case D can be a viable option for efforts in areas where an ensemble run is not possible.

Case Bp has the best result from the ProfDA, which is expected as the calculation is over the target area. This indicates that for Case B the glider data is being phased or masked out with the presence of other data from NCODA.

Case Bf has the best result for the ICfree cases. Introducing the glider data has the strongest result with the presence of ensembles, but Case Df also has a strong showing indicating that the model forecasts are still an improvement.

Table 4: % Differences over Target Area (Time=00Z Analysis)

Mean Difference True vs. False

Treatment	Ensemble	True Error	Forecast Error	Lawnmower	Free	Control
Standard	61.3	62.8	63.6	62.4	53.3	62.8
Glider Profile Data Assimilation	63.3	56.4	60.4	58.3		
Free Running IC's	65.7	60.9	62.1	63.9		

In order to measure forecast skill, the same comparison of true COF minus false COF were performed for the 48hr forecast Fig.14 shows the same increasing trend as was seen with the 00 hour analyses. The glider data improves improves the results over the two week period. Table 5 takes the mean of the differences over the nineteen days and shows a close result for Case B vs. Case E. Case Br shows a very poor result. Limiting the NCODA radius may not have allowed for data to gravitate to capture features that evolved over the forecast time.

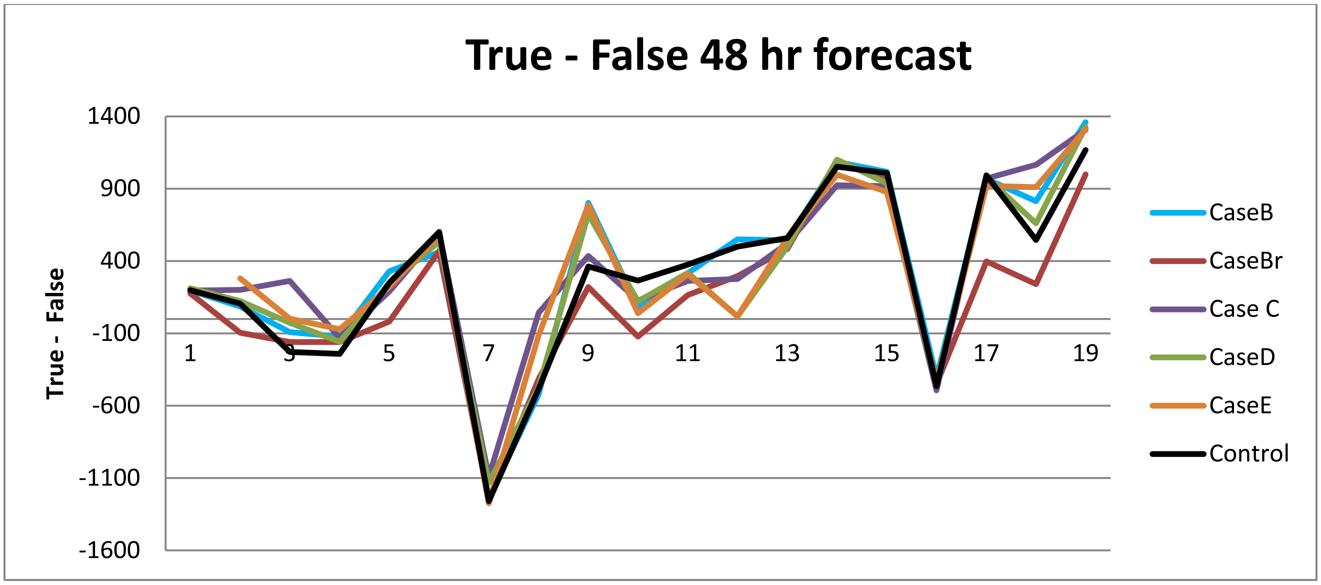

Fig.14 A running calculation of the difference between true and false calculations of cutoff frequency 48 hour forecasts for the original control run spinup OSSE's in the target area.

In the cases where only glider profiles were available for data assimilation, the glider profiles alone do not fill out the whole field as well as other data. Fig. 16 shows a large spread between the performances of all of the cases. The Case Dp result with model data gives a better performance than the Case Bp. As with the Case Br limiting the range of the data over the forecast period, Case Bp may also be too limiting in area coverage for the glider data alone. The Case Cp known error case does best where profiles only are available, but that is to be expected given a known forecast error.

The ICfree cases (Fig. 17) show the highest values in the upward trend over the nineteen days and the highest mean value for the nineteen days. The Case Bf is the best OSSE mean value by a large amount. The value of the TOFU ensemble based cost functions makes a continued impact when other cases are not as strong. The lawnmower case especially drops off toward the end of the 19 days probably from the gliders not capturing important features as the forecast evolves.

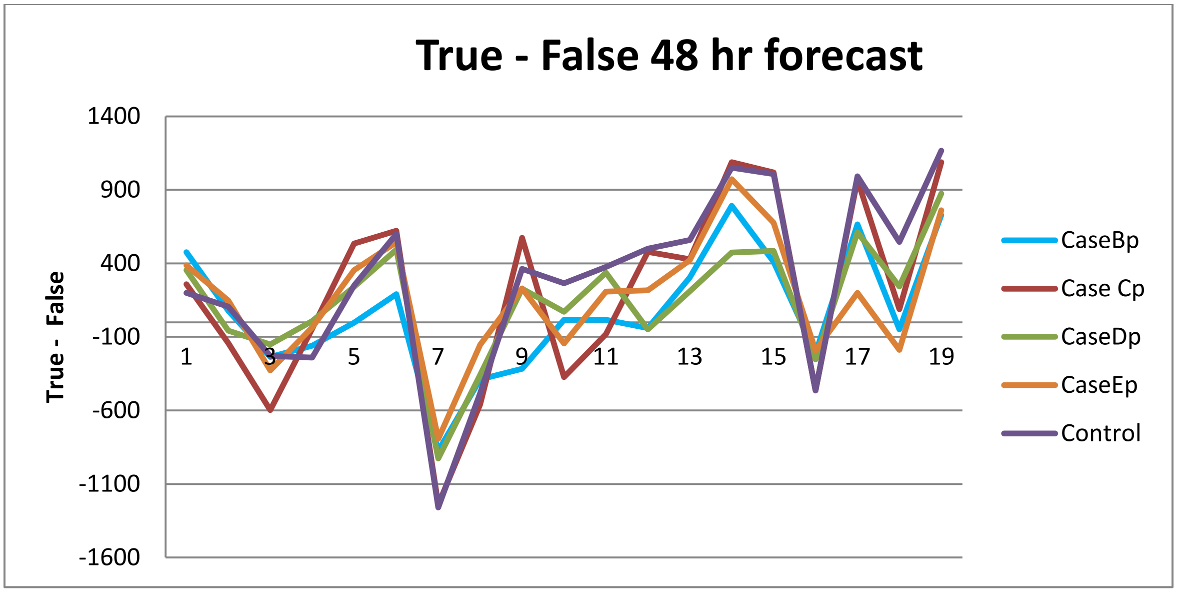

Fig.16 A running calculation of the difference between true and false calculations of cutoff frequency 48 hour forecasts for the glider profile only OSSE's in the target area.

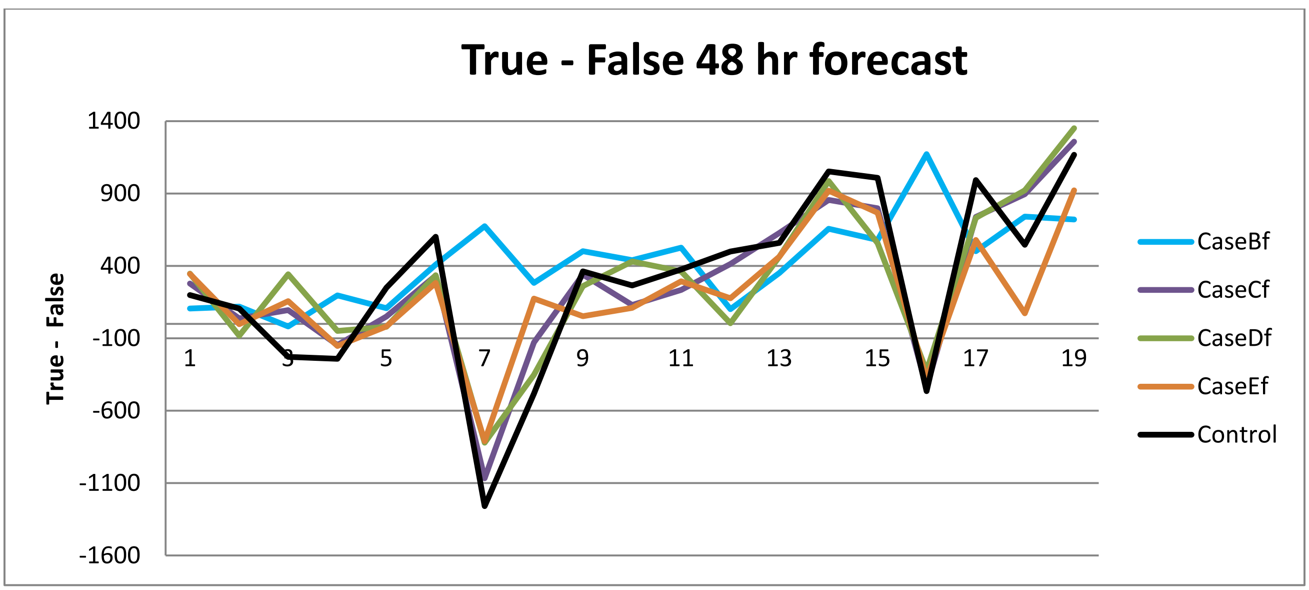

Fig.17 A running calculation of the difference between true and false calculations of cutoff frequency 48 hour forecasts for the free running spinup OSSE's in the target area.

Table 5: % Differences over Target Area (Time=48hr Forecast)

Mean Difference True vs. False

Treatment	Ensemble	True Error	Forecast Error	Lawnmower	Control
Standard	62.0	62.7	60.7	62.1	60.2
Glider Profile Data Assimilation	52.7	57.0	55.5	56.3	
Free Running IC's	65.7	60.2	60.5	57.7	

3.3 Conclusions

The simulated true ocean experiment did not provide the expected results and we could not definitely prefer one criterion for the cost functions over the others. The simulations have been highly affected by NCODA performances. NCODA is effective when there are large (realistic) errors between the assimilated data and forecasted (i.e., the NCODA background) field. In our case, the natrun and contrun (i.e., the initial condition for all experiments) simulations are too similar. Since NCODA extends the influence of the assimilated profile on a radius determined by the correlation length scale, it introduces distortions in the surrounding area of the assimilated profile when the background field is the too close to the true ocean. The problem with the correlation length scale and the too similar background field is confirmed by the CaseBr where the solution is improved by reducing the correlation length scale (ie the radius of influence of the assimilated profiles). Therefore, the cases starting with the free run have the better performance because the data assimilation is effective in correcting the background field and after the initial adjustment the results are comparable with the contrun. Finally, we should not discharge the influence of the extensive interpolation in simulating the glider descending and ascending path.

Moreover, the Okinawa Through region is characterized by high variability and internal wave propagations so that small perturbations may lead to large phase differences in the propagating fields and in the acoustic parameters. Overall, introduction of glider data does improve the OSSE performance. This is supported by the upwards trends of the positive difference in the charts. More analysis needs to be done on the specific use of this data with NCODA. The current system of man in the loop glider guidance can still be utilized. However, as shown in Tables 4 and 5, the GA can outperform the man in the loop scenario. This will be especially useful in situations where many gliders exist and a more automated approach is warranted.

4. MREA_10

The MREA_10 aims to exploit remotely sensed satellite data for (1) extraction of near surface geophysical parameters, (2) utilization of a fleet of gliders (AUVs) to map out the physical and bio-optical properties in the water column prior to and during the cruise, (3) deployment of drifters and HF radar to determine turbulent transport and dispersion, (4) deployment of moorings to initialize and set boundary conditions for atmospheric and oceanic models and finally (5) assimilation and fusion of all data into bio-optical and physical METOC models, providing an integrated approach for near realtime METOC data collection and modeling. The exercise is focused on the littoral zone that is very dynamic and the most difficult area to accurately retrieve remotely sensed geophysical parameters. As part of the project, the NATO Undersea Research Centre (NURC) supported a cruise in the Ligurian Sea to sample similar areas as two previous trials: the Ligurian Sea Cal/Val 2008; LSCV'08 (Oct 2008) and the Battlespace Preparation 2009 (Mar 2009). Slocum coastal gliders were deployed before and during the cruise, but during the trial there have been of an effort to sample specific areas in a 'glider fleet' mode. In support of the modeling efforts, drifters were deployed to track turbulent transport and dispersion in the study area. Two moorings also were deployed to assist in initialization and set boundary conditions for the models and the HF radar study: one mooring was south of Portofino and the other off Palmaria Island.

4.1 The Real Time Exercise

NRLSSC participated in the MREA_10 providing in realtime a full feedback cycle using model prediction to guide the glider and assimilating the collected data back into the model. The goal was to verify how an 'intelligent' guidance of the gliders would improve the forecast skill of the model. The NRLSSC modeling effort was based on the RELO system. Fig. 18 illustrates the model configuration which consisted of 3 nested domains forced by the COAMPS_europe3 surface forcing (Hodur, 1997) and Open Boundary Conditions (OBC) extracted from the simulations of the parent domain. The OBC for the outer most nest were extracted from G8NCOM. Monthly river discharges were from the global river data set of 1/8° Global NCOM (G8NCOM) (Barron and Smedstad, 2002), with the Arno, Magra, and Serchio transports provided by the Istituto Idrografico Italiano. The vertical resolution of each domain had 40 σ- and 10 z-levels (50 levels). The outer nest, nest0, was at 4km horizontal resolution with the primary purpose of serving as a buffer zone between G8NCOM's NOGAPS forcing and the higher resolution wind data set. Nest 1 (2km resolution) included tides. Tides were specified at the boundaries from the Oregon State University tide model (Egbert and Erofeeva, 2002). An ensemble of 32 independent runs of nest1 was also made available in realtime. The simulations were initialized by the Ensemble Transform Kalman Filter (Bishop, *et al*., 2001) using atmospheric forcings perturbed by the space-time deformations method (Hong and Bishop, 2007). Nest2 was about 0.6km resolution and configured for the operational area. While data assimilation was performed on both nest0 and nest1; nest2 was a free run (ie the effects of data assimilation are through the OBC). Then, nest2 may be considered as a dynamical interpolation of nest1 and also served as benchmark for model evaluation and comparison. Data were daily retrieved from both the NRLSSC and NURC data servers.

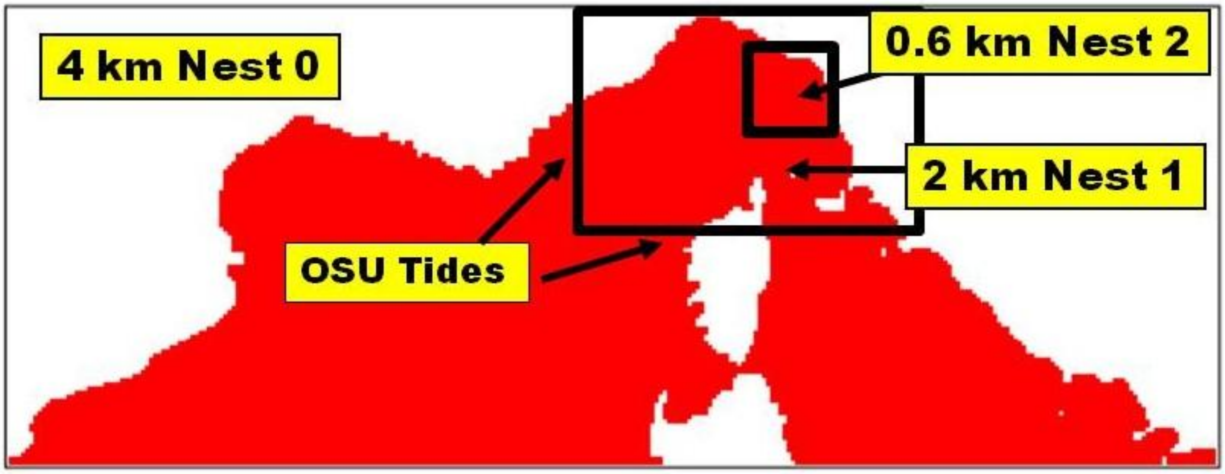

Fig.18 The triple nest configuration for MREA_10.

Although 5 gliders were operating during the exercise, guidance was suggested for and data assimilated from glider LAURA only. This was to verify the impact of few data aimed to improve the forecast in a pre-defined area (ie the target area) vs a broad range of data collected to cover a larger area (ie the operational area). In order to gather more realtime data for NCODA, the analysis time was set at -24 hours and the temperature and salinity innovations inserted between -24 and 0 hrs (henceforth the 0 hours is referred as to as the 0GMT of the current day of the realtime operations). From the analysis, 96 hours of effective forecast (ie, 120 computational forecast) and ensemble runs were provided and the results processed in NetCDF files posted on a user/password protected web page**.** The forecast and ensemble mean and rms were also incorporated in the super-ensemble approach that was run in parallel at NURC (Mourre et al., 2010). The cost function for the GA was derived from the forecast field and ensemble variability and the 48 hour guidance path shared with the NURC glider pilots.

The main issue of realtime operations is a timely delivery of the results. In this exercise we had about 6hr from the availability of the forecast atmospheric fields to the dateline for sending the glider path guidance for the next cycle. To speed up the beginning of the simulations, the -24hr G8NCOM full forecast fields was used to provide OBC to nest0. The full modeling and data model outputs processing cycle was performed at the NRLSSC on dual 64 processors Opteron-based LINUX platforms.

The model simulations started on July 1st 2010 to assess, calibrate the model configuration and to verify the realtime practical applicability. The interactions with glider LAURA were from August 20-28 2010. Fig 19a depicts the surface velocity and temperature field for Aug 25 and Fig 19b the associated ensemble spread. In MREA_10, EMPATH used cost functions based on weighted sums of different constituents including ensemble spreads and specialized acoustic parameters. (Fig 20) (Coelho et al, 2010b). Finally, Fig 21 illustrates the full LAURA track and the delivered paths as computed by EMPATH.

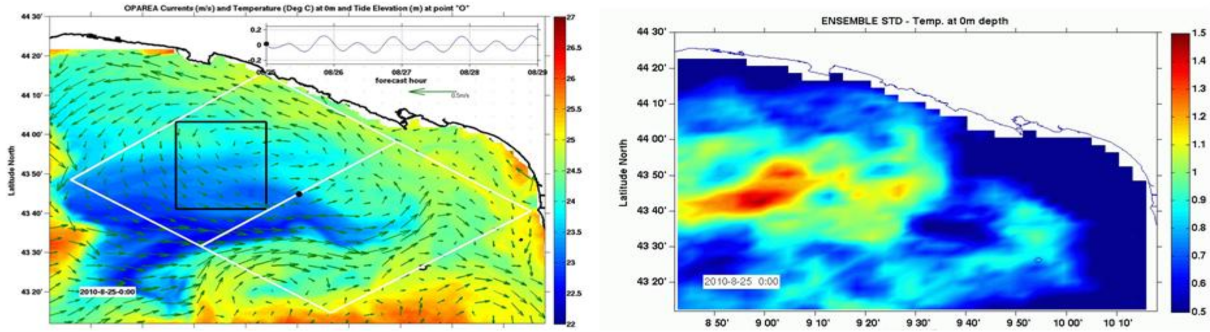

Fig. 19 The surface velocities over the temperature field (a) and ensemble STD for Aug 25. Operational and target areas are delimited in white, and black, respectively.

As outlined in section 2, two sets of constituent cost functions were used in the REP10 adaptive sampling experiment. The first, uses a method based upon the Extended Transform Kalman Filter (ETKF) to determine regions where measurements maximally reduce the forecast uncertainty for a wide range of observables. TOFU products are generated for reduction in uncertainty in temperature, as well as acoustic parameters: Below Layer Gradient (BLG), In-Layer Gradient (ILG), and Sonic Layer Depth (SLD). For this test only Temperature was used. The second set was based upon the ensemble spreads as well as temporal and spatial variability of the model forecast temperature field. The TOFU CF Temperature figure is in the first column, fourth row of Fig. 20. The ensemble spreads at 0, 25 and 100m are shown in the upper row. The spatial variability of the mean T field at the 3 specified depths is in the second row, indicating much more spatial variability at 0 and 25m compared with 100m. The temporal variability of the ensemble-mean field is shown in the 3rd row. The final CF for the uniformly weighted combination (all 1s) of all 10 CCF is shown in the lower right panel.

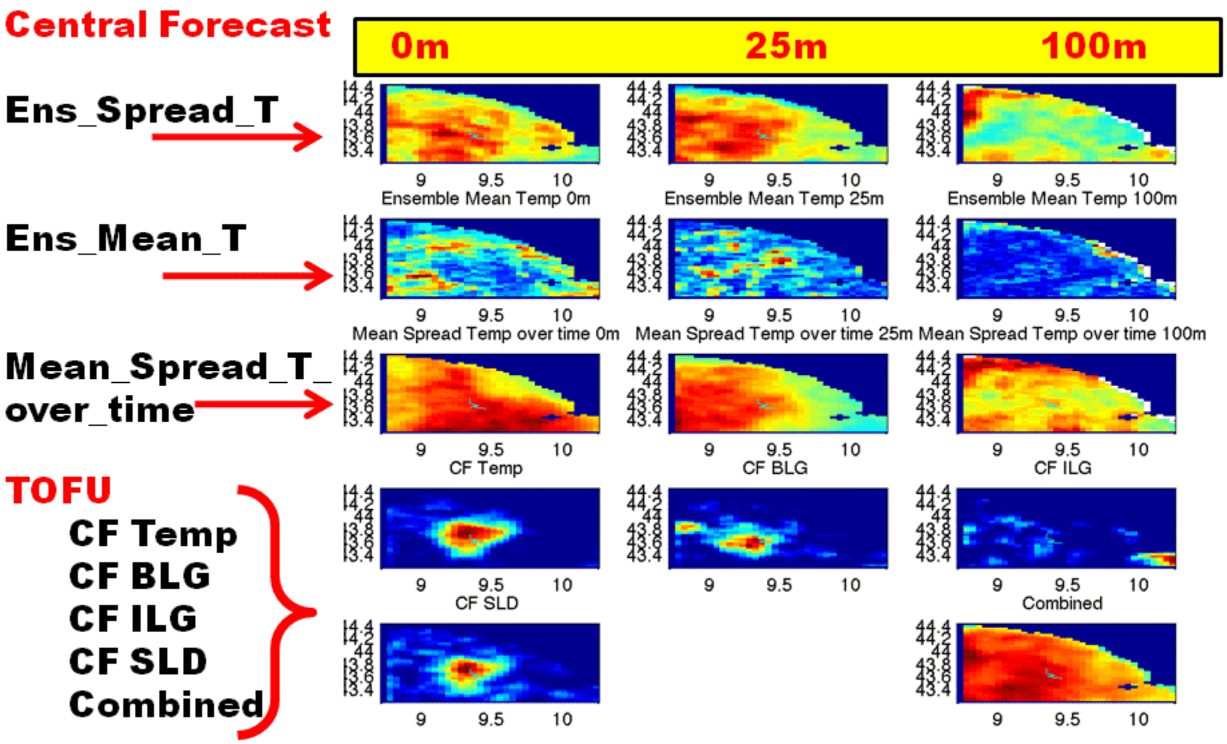

Fig. 20 The input fields to the cost function used by EMPath.

Operationally, EMPath was run daily with a 48 hour forecast. Optimal glider paths were provided to NURC daily, although the navigation was updated every other day. The GA was run with 500 individuals for 80 generations. In order to check convergence and uniqueness of solution it was run 5 times with different random seeds. In order to represent results to the user, an estimated CF morphology is computed. To compute this function, a glider is positioned at each point in the spatial grid and samples the multi-dimensional cost function for 3 hours going North, East, West and South. These are averaged to generate a value of the weighted CF at this point. The solutions are plotted over the CF morphology to provide the user with confidence in the result. Note that the morphology is only a sparse sampling of the extensive time-dependent cost function. The weighting of cost functions was tapered with time. Initial weightings favored the TOFU CF-Temp function due to the emphasis on a target area. As time progressed and the target area became less critical, the relative weighting of the TOFU CF was reduced. Specifically for August 20-23, the weighting went from 12/6/0 for the TOFU with 1 for the 6 ensemble spread CF. This corresponds to a relative weighting of 2-1, 1-1 and 0-1. The 5 best solutions are plotted on the CF morphology in Fig. 21.

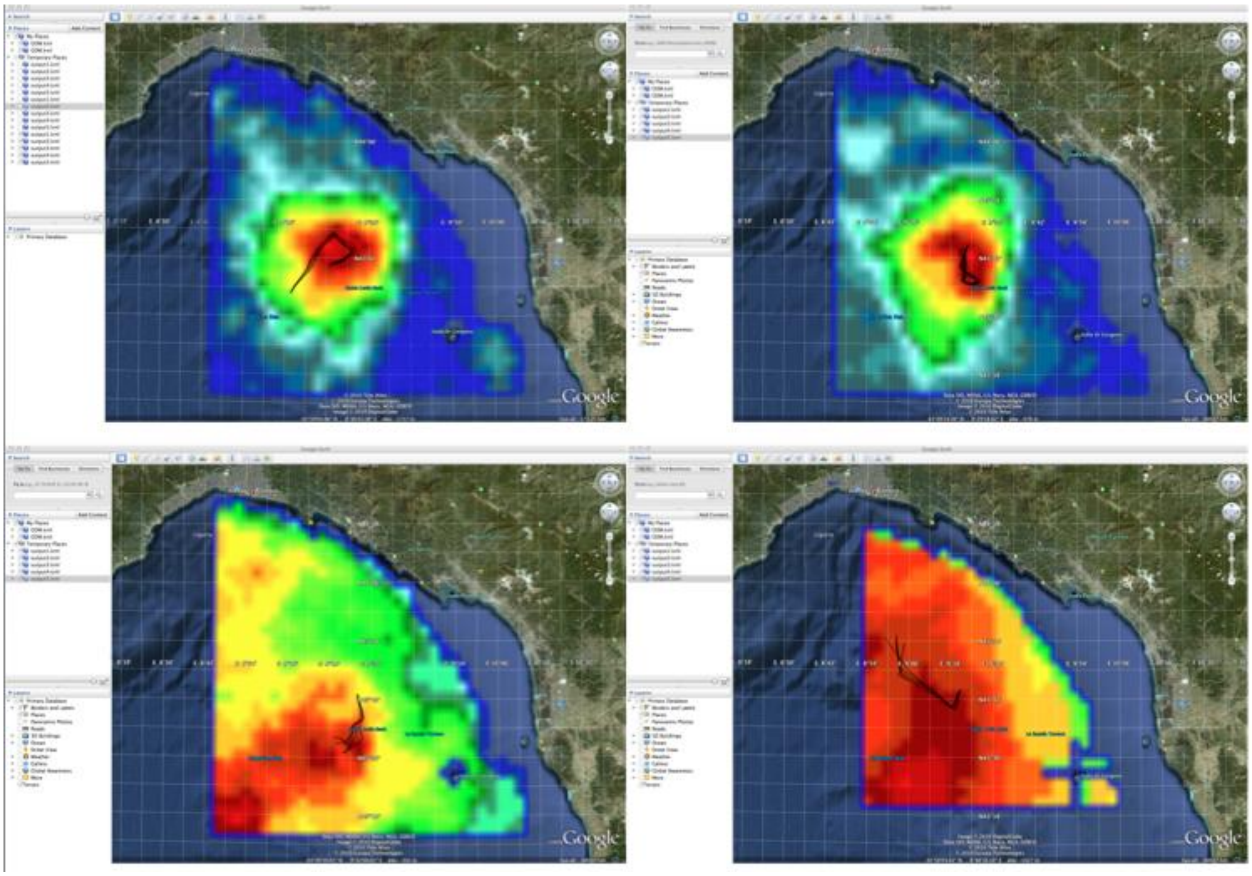

Fig. 21 Morphologies and 5 best GA solutions for Aug 20, 22 and 24. Upper left is 8/24 with a 2-1 TOFU weighting. Upper right is 8/22 with a 2-1 weighting, lower left is the same day with a 1-1 weighting. The lower right panel is 8/24 with a 0-1 weighting.

To illustrate the ability of EMPath to generate glider paths that are achievable within the context of dynamic ocean currents, the left panel of Fig. 22a below shows the input sample guidance (colored lines) overlayed on the actual *Laura* position vehicles for the 6 days of the test. For the first day (red) the guidance started late, so there is a mismatch in the guidance vs. the actual positions. Beyond the north-east corner on day 1 (red), the sampling guidance is exceptionally well executed by *Laura*. The 5 GA solutions for August 24 are shown in the right panel.

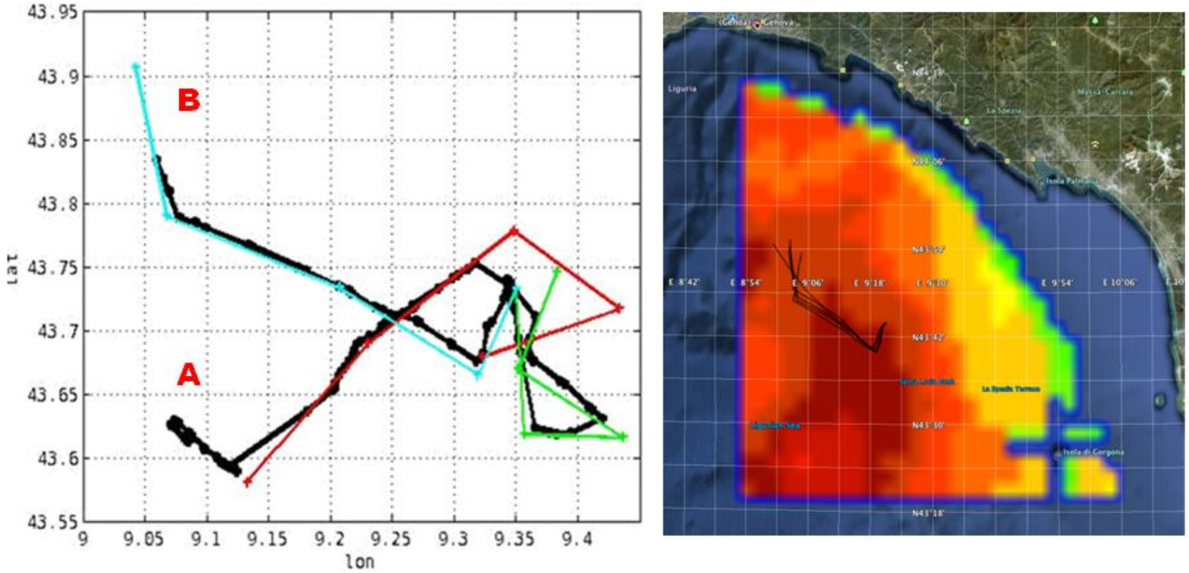

Fig. 22 a) The real track of *Laura* (black) and the different tracks delivered to NURC (colored lines). The points A and B indicates the starting and ending point of *Laura* full path, respectively. b) The morphology function and the best 5 runs for day Aug 24-26.

During the realtime operations, some preliminary evaluation and validation were conducted within the limits of the available not-quality-controlled raw data. Fig 23 illustrates how the data assimilation corrects the position of an eddy on the northern side of the target area. Both figures have identical time stamp, but different forecast hours with respect to two different model cycles. Interactions with NURC confirmed the presence of the eddy at the position indicated by Fig 23 (Alvarez, personal communication).

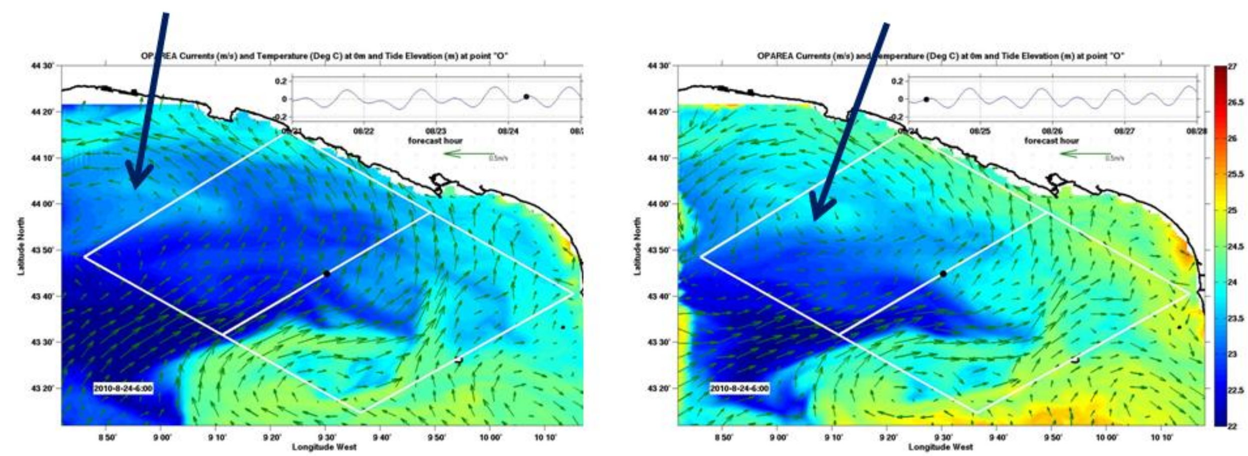

78hr forecast from 2010082100 6hr forecast from 2010082400

Fig 23. Snapshot images of surface velocities over temperature for 2010082406 as forecasted a) at the early stages of assimilating the glider profiles, August 21st and b) after a few assimilating cycles, August 24th.

Fig. 24 indicates how the forecast errors were dramatically reduced in the target area as the LAURA data were inserted in the model forecast cycle. We have computed the RMS error between the data collected inside the target area and the profile from the closest points (in time and space) of the cycle first 48hr forecast. The data for the comparison were not assimilated in the day of the evaluation. As expected, the inner higher-resolution free nest is initially more accurate than the outer nest, but as the assimilation of the glider data starts, the outer nest errors are reduced and a few assimilating cycles are needed for transmitting the correction into the inner domains.

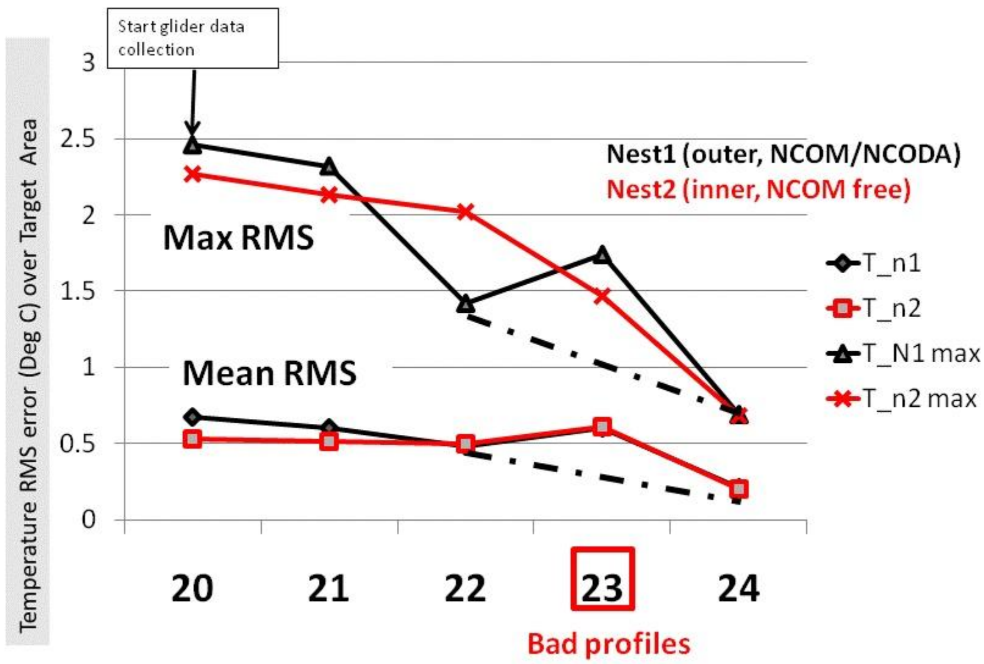

Fig. 24 The max and mean RMS value of the error between observations and model solutions in the target area . Nest1 (black), nest2 (red).

4.2 The Reanalysis

After the completion of the realtime exercise, two parallel experiments were conducted simulating the 'realtime' mode: 1) assimilating data collected by ***all*** the 5 gliders (henceforth referred as to as Allgliders or Allgl) and 2) assimilating ***all but*** LAURA data (henceforth referred as to as Nolaura or NoLr). The simulations assimilating LAURA only are henceforth referred as to as Realtime or Realt. Fig 25 illustrates the number of profiles assimilated in each cases. The difference in number is quite relevant and it should be taken into consideration when comparing and evaluating the 3 experiments. Unfortunately we had no control on the observations accepted by NCODA. As Fig 25 indicates Allgl is not assimilating all the Realt profiles nor all NoLr profiles, but it is important to note that Realt is assimilating one order of magnitude less profiles than the other cases.

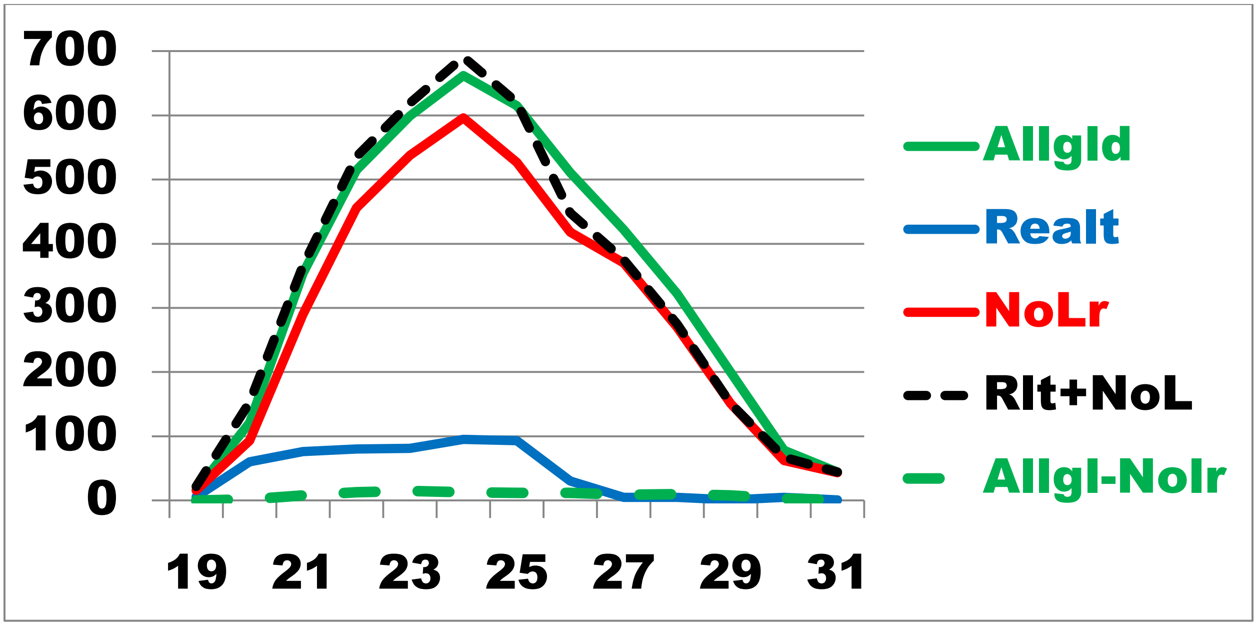

Fig 25. The number of profiles assimilated in the experiments. i) Allglider (green), ii) Realt (blue), iii) NoLr (red), iv) Realt + NoLr (dashed black line) v) Allgl – NoLr (dashed green line).

Data for the new experiments have been retrieved during the operations at sea; therefore, they have the same no-quality-control issues of the Realt simulations, leaving NCODA to discharge 'bad' measurements. On the other hand, the new model-data comparison has been conducted with the quality-controlled observations that NURC has made available after the conclusion of the exercise. This new data set also includes the CTDs collected by the *NR/V Alliance.*

Fig. 26 compares one profile with the solution of two different forecast cycles and Fig 27 (right) depicts the RMS errors as function of depth at an early stage of the assimilation (Aug 21st) and after a few assimilating cycles (Aug 25th). As expected, at the beginning all nests have similar error distribution with the inner high-resolution nests being more accurate. However, as the assimilation continues, the error of the outer nest is reduced with a greater gain in the upper levels. The Allglider experiment is also more accurate at the thermocline. We can deduce that Realtime lacks of information outside the area sampled by LAURA that can propagate the analysis correction inside the target area and NoLaura experiment lacks of observations aimed to improve the forecast in the target area.

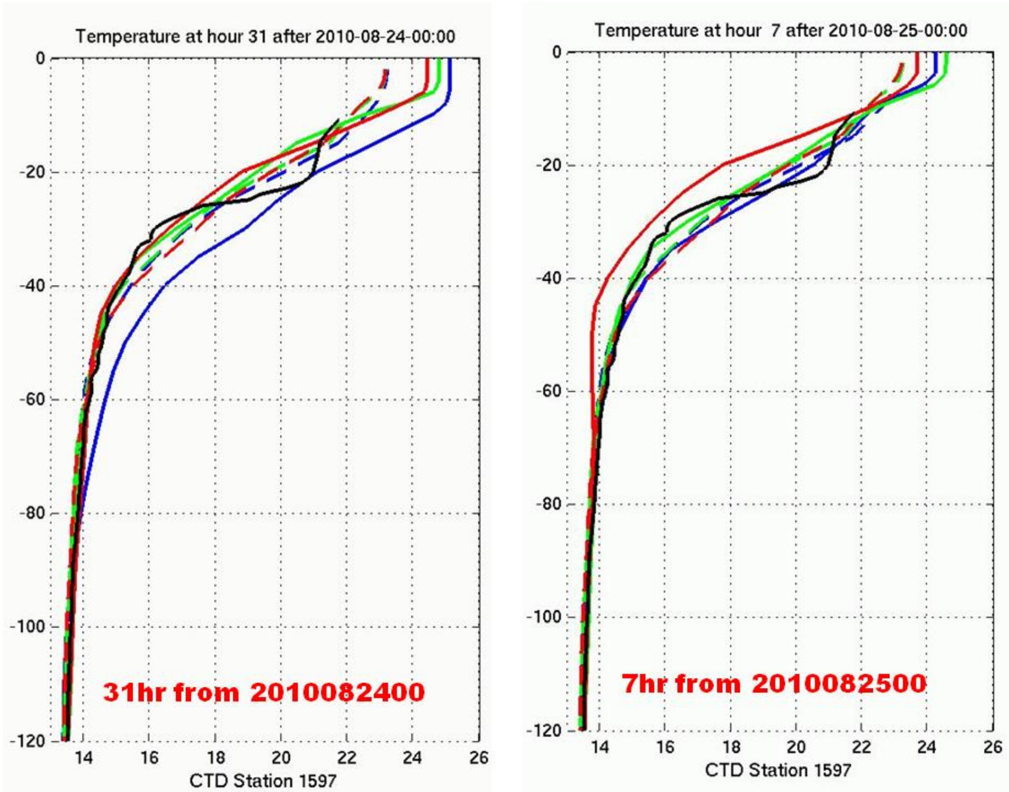

Fig 26. Model-data comparison for CDT 1597 at (9.28E, 43.7N) on Aug 25, 06:58. a) cycle 2010082400 forecast 31hr, b) cycle 2010082500 forecast 7hr. Nest1 (solid line) and Nest2 (dashed lines). Realt (blu), Allgl (green), NoLr (red).

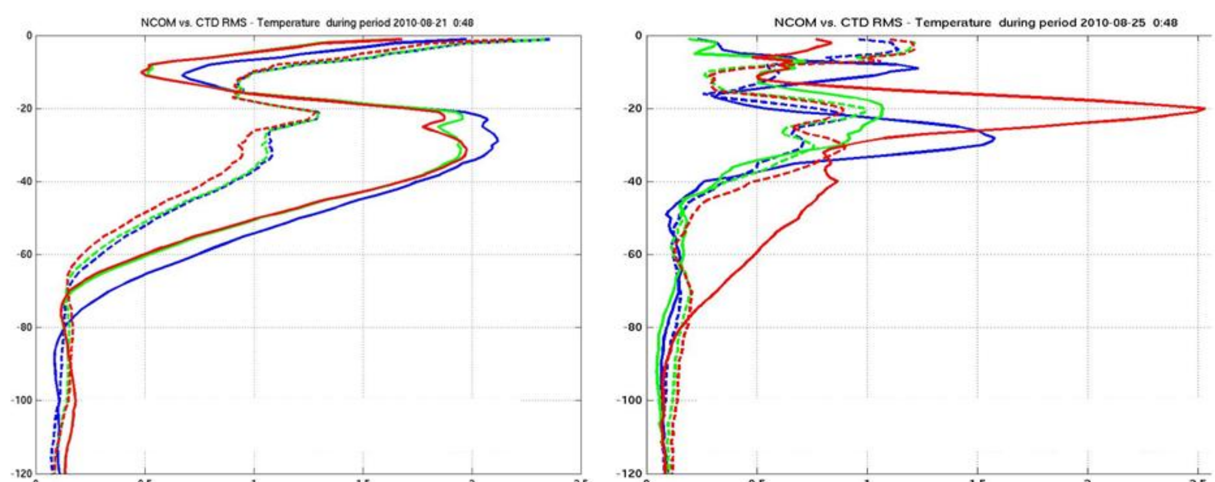

Fig 27. The RMS error between the model and the profile collected in the target area in the the first 48 forecats .

One of the main issues in these data assimilation experiments is how to remove the bias, especially at the lower depths un-sampled by the gliders. To evaluate the impact of the assimilation on correcting the background bias, we have computed the distribution of the error between data and models (Fig 28 a-c) and then computed the best fit 5^{th} order polynomial, P5, of each histogram (Fig. 28d). Let x_{max} and x_{efold} the points such as: $P5(x_{max})$=max and $P5(x_{efold})$= 0.5 $P5(x_{max})$. Therefore, x_{max} and x_{efold} are representative of the background bias and decay of the error, respectively. Fig 32 illustrates the evolution of the mean (over depth) bias during the exercise. Toward the end of the trial, very few data were collected inside the target area and after Aug 26^{th} the graphic may not be statistically representative. Hower, it is evident that the background bias is sensibly redured for all the experiments and all domains.

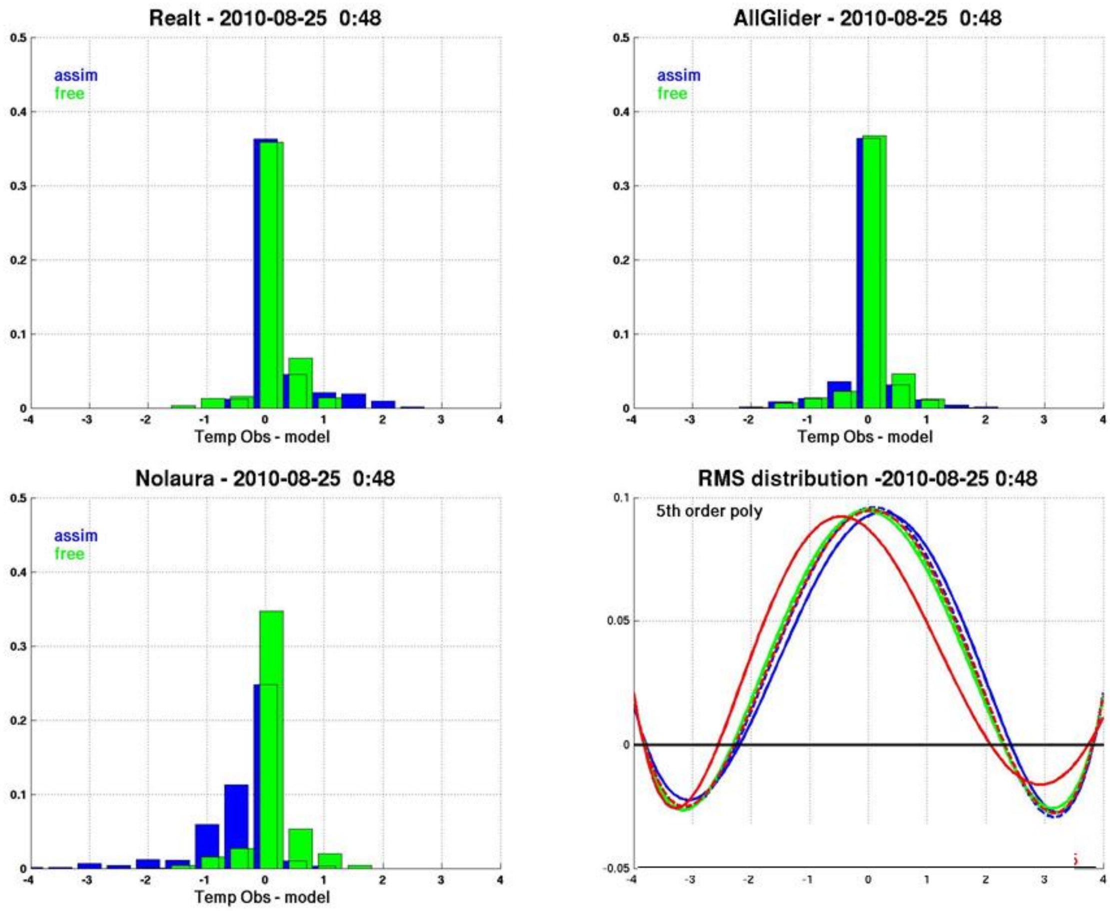

Fig. 28 The errors between data and model 48hr forecast for day August 25^{th}: nest1 (blue) and nest2 (green). a) Realt b) Allgl, c) NoLr, and d) best fit of the histograms on a 5^{th} order polynomial. See text for explanations of terms

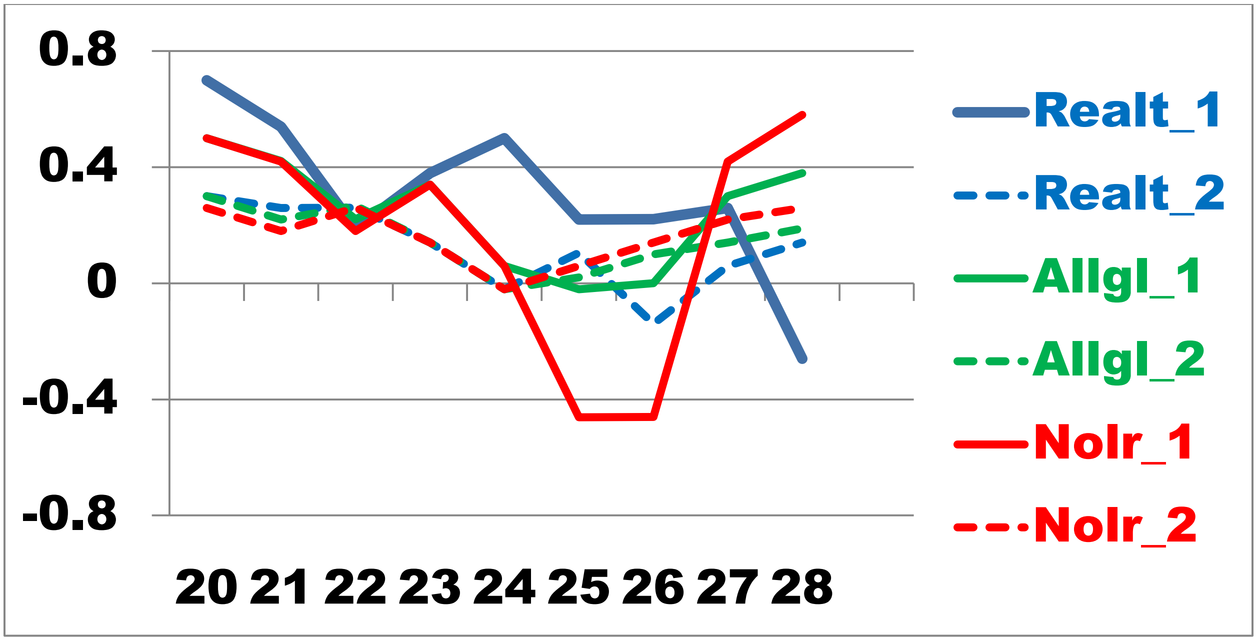

Fig 29. The background bias of the model simulations as function of time. Nest1 (solid line) Nest2 (dashed line). See text for definition of terms.

4.3 Conclusions

We have conducetd a realtime exercise in which the ocean model forecast and ensemble variability served as input to and a Genetic Algorithm to provide guidance to gliders and the collected data were assimilating back into the model. Even though 5 gliders were deployed during the trial, only one glider, LAURA, was guided and her (?) collected data assimilated. The experiment was quite successful indicating the practical feasibility of the procedure and how an 'intelligent' sampling can sensibly reduce the forecast errors in a target area.

We also have conducted parallel experiments assimilating all the available gliders and all but LAURA data. In general, the Allgl has the best performance and assimilating more data in the operational area and the NoLaura high number of profiles reduces the errors and the correction from the data are propagating inside the target area. On the other side an aimed and 'intelligent' guidance of only one glider provide the same kind of accuracy with at least one of order of magnitude of collected data.

5. Summary

This document is designed to evaluate the impact of the EMPath Genetic Algorithm in the adaptive sampling strategies to direct and guide gliders during realtime operations. EMPath has been successfully interfaced with the RELO forecast system and applied with several criteria and approaches in defining the driving cost function. The validation tests have been designed to verify the skills and limits of the several approaches and document the results of a realtime exercise, MREA 10.

Altough the OSSE experiment did not provide a clear indication of the differences between the several approaches, it cannot be forgotten that application of each criteria should take into consideration the goals and aims of the operation. The ensemble approach is most indicated in realtime operations in limited areas where there is a clear need of improving the forecasting skill of the model in a limited area and reducing the errors in derived variables such as the acoustic properties of the area. The MREA10 is a clear demonstration where few data from a well-directed glider had comparable impact of assimilating many more observations.

When the goal is mainly to improve the forecast at a meso/regional scale, it may be preferable to adopt the less computational intensive approach based on the forecast error. Finally, the lawnmower approach is well suitable for long terms surveys in areas where the impact of the assimilated data may propagate well outside the operational area.

6. Acknowledgements The authors would like to thank Jan Dastugue of NRLSSC for help with graphics and Bob Helber of NRLSSC for the COF and SLD routines, and David Sitton of Qinetiq North America for help with making ETATM files from the TOFU. This work is funded through the Space and Naval Systems Warfare Command PEO C4I and PMW 120.

7. Technical References

Barron, C. N., R. W. Helber, G. A. Jacobs, M. Gunduz, and P. Spence, 2009: Acoustic impact of short-term ocean variability in the Okinawa Trough. Proceedings, OCEANS 2009 MTS/IEEE Biloxi, 29-29 October 2009, Biloxi, MS.

Barron, C.N., A.B. Kara, P.J. Martin, R.C. Rhodes, and L.F. Smedstad, 2006: Formulation, implementation and examination of vertical coordinate choices in the Global Navy Coastal Ocean Model (NCOM). *Ocean Modelling*, **11**, 347-375.

Barron, C.N. and L.F. Smedstad, 2002: Global River Inflow within the Navy Coastal Ocean Model. Proceedings, MTS/IEEE Oceans 2002 Conference, 29 October 2002, Biloxi, MS, 1472-1479.

Bishop,C.H., B.J. Etherton, and S.J. Majumdar, 2001: Adaptive Sampling with the Ensemble Transform Kalman Filter. Part I: Theoretical Aspects. *Mon. Wea. Rev*., **129**, 420-436.

Coelho, E.F., J.P Fabre, C. Rowley, C.H. Bishop, G. Jacobs, J. Cummings, and X. Hong, 2010a: Targeting observations to reduce acoustic prediction uncertainty. *U.S. Navy Journal of Underwater Acoustics*, **60,** Nr.1.

Coelho, E.F., Rowley, C., Bishop, G.H., Fabre, J.P., Sitton, D., Jacobs, G., Cummings, J., Hong, X., Peggion, G., 2010b: Target Observations Using Forecast Uncertainties - Validation Test Report. Naval Research Laboratory, NRL/MR/7320--10-9245.

Cummings, J. A., 2005: Operational multivariate ocean data assimilation. *Quart. J. Royal Met. Soc.*, **131**, 3583–3604.

Egbert, G. and L. Erofeeva, 2002: Efficient inverse modeling of barotropic ocean tides. *J. Atmos. Oceanic Technol.*, **19**, 183-204.

Fritsch, F.N. and R.E. Carlson, 1980: Monotone Piecewise Cubic Interpolation. SIAM J. Numerical Analysis 17, pp. 238-246,

Gerstoft,P., 1994: Inversion of siesmoacoustic data using genetic algorithms and a posteriori probability distributions,*Journal of the Acoustical Society of America*, **95(2),** 770-782.

Gerstoft. P. and D. F. Gingras; 1996: Parameter estimation using multifrequency range-dependent acoustic data in shallow water. *Journal of the Acoustical Society of America*, **99(5)**, 2839-2850.

Goldberg, D.E., 1989: *Genetic Algorithms in Search, Optimization and Machine Learning*, (Addison-Wesley, Boston).

Heaney, K.D., and H. Cox, 2006: A tactical approach to environmental uncertainty and sensitivity. IEEE Journal of Oceanic Engineering, 31, 356-367.

Heaney, K.D., G. Gawarkiewicz, T.F. Duda, and P.F.J. Lermusiaux, 2007: Nonlinear optimization of autonomous undersea vehicle sampling strategies for oceanographic data-assimilation. Journal of Field Robotics, 24, 437–448.

Heaney,K.D., R. L. Campbell, R.H.Stroop, L.F. Smedstad, and G. Peggion, 2012: Environmental Measurements Path Planner (EMPath) Users Manual, *NRL Report* NRL/MR/7320--12-9359.

Helber, R.W., C.N. Barron, M. Gunduz, P.L. Spence and R.A. Zingarelli, 2010: Acoustic metric assessment for UUV observation system simulation experiments. *U.S. Navy Journal of Underwater Acoustics*, **60**, 101-124.

Hodur, R. M., 1997: The Naval Research Laboratory's Coupled Ocean/Atmosphere Mesoscale Prediction System (COAMPS). *Mon. Weather Rev.*, **125**, 1414–1430.

Hogan, T., and Rosmond, T., 1991: The description of the Navy Operational Global Atmospheric Prediction Systems spectral forecast model. *Mon. Weather Rev.*, **119**, 1786–1815.

Hong, X. , and C.H. Bishop,"Ensemble and Probabilistic Forecasting", 2007. In Proceedings *IUGG XXIV General Assembly 2007*, Perugia, Italy, 2-13 July (2007).

Kahaner, D., C. Moler, and S. Nash, 1988: *Numerical Methods and Software*, Prentice Hall.

Majumdar, S.J., C.H. Bishop, B.J. Etherton and Z.Toth, "Adaptive Sampling with the Ensemble Transform Kalman Filter. Part II: Field Program Implementation". Mon. Wea. Rev., 130, 1356-1369 (2002).

Martin. P.J., C. N. Barron, L. F. Smedstad, T. J. Campbell, A. J. Wallcraft, R. C. Rhodes, C. D. Rowley, T. L. Townsend and S. N. Carroll, 2009: User's Manual for the Navy Coastal Ocean Model (NCOM) version 4.0 *NRL Report* NRL/MR/7320--09-9151.

Masutani, M., T.W. Schlatter, R.M. Errico, A. Stoffelen, E. Andersson, W. Lahoz, J.S. Woollen, G.D. Emmitt, L.P. Riishojgaard, and S.J. Lord, 2010: Observing system simulation experiments. *Data Assimilation: Making Sense of Observations*, W. Lahoz, B. Khattatov, and R. Menard, Eds., Springer, 647-679.

Memorandum 3100 COO/022 16Mar 2007, Modeling and automation requirements in support of the Naval oceanography operations command.

Memorandum 3140 Ser N84/9U176518 4Feb09, Fiscal year 2010 (FY10) Guidance for meteorology and oceanography (METOC) research and development projects.

Mourre, B., J. Chiggiato, F. Lenartz, and M. Rixen, 2010: Uncertainty forecast from 3-D super-ensemble multi-model combination: validation and calibration. Ocean Dynamics 62(2) 283-294.

Rowley, C., 2010: Validation Test Report for the RELO System. Nav. Res. Lab., Stennis Space Center, MS, NRL MR 7320-10-9216. 69 pages.

Rowley, C., P.J. Martin, and J.A. Cummings, 2009: The Naval Research Laboratory Relocatable Ocean Nowcast/Forecast System. *U.S. Navy Journal of Underwater Acoustics*, **60**(1), 169-202.

Zingarelli, R.A. and J.P. Fabre. 2009: Operational acoustic transmission loss uncertainty characterization. *2009 NRL Review* 130-131.

8. Acronyms

Acronym	Description
ASCII	American Standard Code for Information Interchange
CFL	Courant Fredrich Levy scheme
CF	Cost Function
CCF	Constituent Cost Function
COAMPS	Coupled Ocean Atmosphere Mesoscale Prediction System
COF	Cutoff Frequency
DoD	Department of Defense
EMPath	Environmental Measurements Path Planner
ETKF	Ensemble Transform Kalman Filter
G8NCOM	1/8^{o} Global NCOM
GA	Genetic Algorithm
GDEM	Generalized Digital Environmental Model
GOST	Glider Observation Sampling Strategies
GUI	Graphical User Interface
IAMPS	Integrated Acoustic Multienvironmental Processing System
ILG	In-Layer Gradient
METOC	Meteorological and Oceanographic
MREA10	Maritime Rapid Environmental Assessment of 2010
NAVO	Naval Oceanographic Office
NCODA	Navy Coupled Ocean Data Assimilation
NCOM	Navy Coastal Ocean Model
NOGAPS	Navy Operational Global Atmospheric Prediction System
NRL	Naval Research Laboratory
NRLSSC	Naval Research Laboratory - Stennis Space Center
NetCDF	Network Common Data Form
NURC	NATO Undersea Research Centre
OBC	Open Boundary Conditions
OSSE	Observation System Simulation Experiment
RELO	Relocatable Circulation Prediction System
RMS	Root Mean Square
SLD	Sonic Layer Depth
TOFU	Target Observations Using Forecast Uncertainties
UAVs	Underwater Automated Vehicles
VTR	Validation Test Report